NASA TECHNICAL NOTE

NASA TN D-3621

c.1

NASA TN D-3621

LARGE-SCALE WIND-TUNNEL TESTS OF A LOW-ASPECT-RATIO DELTA-WINGED MODEL EQUIPPED WITH SHARP-EDGED STRAKES

by Victor R. Corsiglia and David G. Koenig

Ames Research Center
Moffett Field, Calif.

NATIONAL AERONAUTICS AND SPACE ADMINISTRATION • WASHINGTON, D. C. • SEPTEMBER 1966

LARGE-SCALE WIND-TUNNEL TESTS OF A LOW-ASPECT-RATIO DELTA-WINGED MODEL EQUIPPED WITH SHARP-EDGED STRAKES

By Victor R. Corsiglia and David G. Koenig

Ames Research Center
Moffett Field, Calif.

NATIONAL AERONAUTICS AND SPACE ADMINISTRATION

For sale by the Clearinghouse for Federal Scientific and Technical Information
Springfield, Virginia 22151 – Price $2.50

LARGE-SCALE WIND-TUNNEL TESTS OF A LOW-ASPECT-RATIO DELTA-WINGED MODEL EQUIPPED WITH SHARP-EDGED STRAKES

By Victor R. Corsiglia and David G. Koenig
Ames Research Center

SUMMARY

A wind-tunnel investigation was made to determine the longitudinal stability, lift, and landing and take-off performance of a delta-wing configuration equipped with strakes. The model was a wing, fuselage, vertical-tail combination. Four wing strake configurations were investigated. Some data were obtained with the model in the proximity of the ground.

The strakes were found to increase lift coefficient significantly at angles of attack, above about 12°. However, the increase in lift coefficient was accompanied by a reduction of static longitudinal stability.

INTRODUCTION

One of the problems in the design of fixed wing aircraft for supersonic flight speeds is the low lift-curve slope for low-aspect-ratio wings. Studies at small scale (refs. 1-3) have shown that a free-vortex flow generally occurs near the leading edge of delta wings of low aspect ratio. This flow results in higher experimental lift-curve slopes than those predicted by potential flow theory. The investigation reported in reference 4 indicated that lift-curve slope could be increased further by the addition of a highly swept strake to the inboard portion of a delta wing to form a double delta planform.

An investigation has been undertaken at large scale to determine the longitudinal aerodynamic characteristics of an airplane configuration having a double delta wing. In particular, it was desired to determine the effect of various strake configurations on longitudinal stability, lift, and landing and take-off performance. The model was equipped with leading- and trailing-edge flaps. A limited amount of testing was done with slots and leading-edge flaps installed on the strakes and with the model in the proximity of the ground.

NOTATION

A aspect ratio, $\frac{b^2}{S}$

A' aspect ratio, $\frac{b^2}{S'}$

b span, tips off, ft

c chord, ft

$\bar{c}$ mean aerodynamic chord, $\frac{2}{S}\int_0^{b/2} c^2\,dy$, ft

c_R root chord, extension of wing leading edge and trailing edge to fuselage center line

C_D drag coeeficient, $\frac{D}{qS}$

C_L lift coefficient based on total wing area not including strake area, $\frac{L}{qS}$

C_L' lift coefficient based on total wing area including strake area with C_{L_o} subtracted from the measured C_L, $\frac{L}{qS'}$

C_m pitching-moment coefficient, $\frac{M}{qS\bar{c}}$

D drag, lb

h height of moment center above the ground, ft

L lift, lb

M pitching moment about the $\bar{c}/4$ station, ft-lb

q free-stream dynamic pressure, lb/sq ft

S total wing area, 446 sq ft, strakes off, tips on

S' total wing area including strake area, tips off

T thrust, lb

V airspeed, knots

α angle of attack of the wing reference line, deg

δ_f trailing-edge-flap deflection, normal to hinge line, deg

δ_n deflection of leading-edge flap on basic wing, normal to hinge line, deg

δ_{n_s} deflection of leading-edge flap on strake, normal to hinge line, deg

Λ_s strake leading-edge sweep angle, deg

λ taper ratio, $\frac{\text{tip chord}}{c_R}$

η_{IB} spanwise station of intersection of the strake leading edge and basic wing leading edge, based on semispan, tips off

Subscripts and Abbreviations

TE trailing edge

LE leading edge

u uncorrected

o conditions at zero angle of attack

LO conditions at lift off

α flow angularity in wind tunnel

MODEL AND APPARATUS

Figure 1 is a photograph of the model with the $A = 1.34$ wing and the 77° swept strake installed on the ground plane support system. The characteristics of the airplane in proximity to the ground were obtained by lowering the model toward the wind-tunnel floor.

The model consisted of a delta-wing fuselage and vertical-tail combination, identical to that of reference 5, with strakes added to form the double delta planforms. Details of the basic delta-wing model are shown in figure 2(a) and table I, and the dimensions of the four strake configurations are given in figure 2(b). As shown on figure 2(a), the wing was equipped with leading- and trailing-edge plain flaps. The locations of the hinge lines of the flaps are shown on figure 2(c). Unless otherwise noted, the leading-edge flap was deflected only on the portion of the leading edge outboard of the strakes. The strake leading edge was deflected with the smaller 77° strake only. The entire leading edge of all planforms was sharp. The 59° delta wing had an NACA 0003-03 section, and the strake had a wedge leading-edge section (fig. 2(c)).

For part of the test, slots were cut through the strakes in an attempt to improve the longitudinal stability of the configuration. Details of the slots in the smaller and larger 77° strakes are shown in figure 2(d). For the smaller strake the slot area was 0.0061 S, and for the larger strake the area of slot A was 0.011 S. The areas of slots B and C were one-half and one-fourth of the area of slot A, respectively. These slots were closed unless noted otherwise. As shown on figure 2(d) a streamwise notch was also tested at the juncture of the basic wing and the strake leading edge.

TEST PROCEDURE AND CONDITIONS

The angle of attack of the model was varied from -2° to $+22^{\circ}$ at zero sideslip. For all the tests the ground plane was installed. Most of the tests were made with the model in the highest position ($h/\bar{c} = 0.66$). With the proper wall corrections applied to the data these tests are representative of out-of-ground-effect conditions. Some of the configurations were tested closer to the ground plane of the test section to determine ground effects. A list of the configurations investigated is shown in table I. The Reynolds number, based on the mean aerodynamic chord of the basic delta wing, was 13.7×10^6, the Mach number was 0.10, and the free-stream dynamic pressure was 15 psf.

DATA REDUCTION AND CORRECTIONS

Force and moment data were measured with a mechanical scale system. The reference area for all force and moment coefficients, unless otherwise noted, is that of the basic delta wing ($S = 446\ ft^2$).[1] The only exception to this procedure is the theoretical and experimental comparisons presented in figure 20. Since the aspect ratio is a prime variable in the theory, the experimental data were not corrected for aspect-ratio effects by the procedure given in footnote 1. The reference length for moment coefficient is the mean aerodynamic chord ($\bar{c} = 19.1$ ft), and moments are taken about $0.25\bar{c}$. The area, length, and moment center location are all based on the basic delta wing with the tips on.

The following strut tares and wind-stream angularity corrections have been applied to all the data:

$$\alpha = \alpha_u + \alpha_\alpha$$

$$C_L = C_{L_u} + (\Delta C_L)\ \text{tare} - C_{D_u} \sin \alpha_\alpha$$

$$C_D = C_{D_u} + (\Delta C_D)\ \text{tare} + C_{L_u} \sin \alpha_\alpha$$

$$C_m = C_{m_u} + (\Delta C_m)\ \text{tare}$$

The strut tares corresponded to force and moment data taken with no model in the wind tunnel.

[1]It should be noted that basing the lift coefficient upon S rather than S' is equivalent to basing the lift coefficient upon S' and making a first-order correction for changes in aspect ratio

$$C_L = \frac{L}{qS} = \frac{L}{qS'}\frac{S'}{S} = \frac{L}{qS'}\frac{A}{A'}$$

since the span does not change and lift is proportional to aspect ratio. This procedure allows direct comparison of the data obtained with planforms of varying aspect ratio.

No wind-tunnel wall corrections were applied to the data presented as being characteristic of conditions in the proximity of the ground. Previous experience has shown that data obtained for the model with the ground plane at the upper ground height ($h/\bar{c} = 0.66$) are characteristic of the out-of-ground-effect condition ($h/\bar{c} \to \infty$), providing the usual wind-tunnel wall corrections are applied. The corrections are

$$\Delta\alpha = 1.06 \, C_L$$

$$\Delta C_D = 0.0184 \, C_L^2$$

RESULTS AND DISCUSSION

Table II lists the figures presented in this report. Lift, drag, and pitching-moment data are presented in figures 3 through 15. Data for the basic wing without strakes are shown in figures 3 and 13. Figures 3, 4, and 5 show the effect of tips, which were off unless otherwise noted.

Effect of Strake Sweep and Size on the Lift and Pitching-Moment Characteristics

Lift.- Figure 16 presents a summary of the effects of strake configuration on lift. The lift coefficients, which are based on the wing area of the basic delta planform, are identical to those based on the actual wing area and then corrected by the ratio of the aspect ratios (see Data Reduction and Corrections section).

It can be seen in figure 16(a) that the addition of strakes caused a significant increase in C_L over the basic wing for angles of attack above 12°, but the increase is smaller at angles of attack below 12°. It can also be seen that the lift is increased by the larger strakes (lower aspect ratio) and is not affected significantly by the sweep angle of the strake leading edge.

Deflecting the nose flaps to 30° reduced C_L at 12° angle of attack by about 0.07 to 0.12, depending on the planform, as may be seen by comparison of figures 16(a) and 16(b).

Figure 17 shows the effect of proximity to the ground on lift for the configuration with the higher aspect ratio and higher sweep. At a ground height of $h/\bar{c} = 0.32$, the increment of C_L due to ground effect is about 25 percent higher than the lift increment due to the ground of the basic wing. This increment of C_L due to ground effect for the strake-on configuration is 0.18 at 12° angle of attack.

Pitching moment.- Figure 18 is a summary of the moment characteristics for the strake-on configurations. It is seen that the linearity of the pitching moment is adversely affected by increasing strake size (reducing aspect ratio). With the nose flaps undeflected the aerodynamic center moved forward from its location at zero lift approximately 3 and 8 percent for the smaller and larger strakes, respectively. The use of leading-edge flaps deflected to 30° made the pitching-moment curves more linear, but decreased the static margin from its value without nose flaps for C_L from 0.2 to 0.6 (landing and take-off values). A possible explanation is that the leading edge of the basic wing outboard of the strakes was deflected, with the result that the leading-edge separation was suppressed; hence there is less vortex induced lift on the outboard portion of the wing, which is generally aft of the moment center. This explanation is supported by noting in figure 18 that at $C_L = 0.4$ the reduction in static stability caused by nose flaps is more extensive with the larger strakes (lower aspect ratio), where the nose flaps cover a smaller portion of the total span and the centroid of the wing area affected has moved farther aft. Also the results shown in figure 10 indicate that when the nose flaps are extended over the entire span of the wing, the static stability is not reduced by nose flap deflection.

The slot in the 77° strake, as seen in figure 10, improves the static stability an amount approximately equal in magnitude to the improvement due to deflecting the full-span leading-edge flaps to 30°.

The change in trim requirements as the ground is approached is shown in figure 19. The data for the basic wing with tips on are compared to the data obtained with strakes on. It is seen that the effect of proximity of the ground on the change in C_m is 25 to 35 percent less for the model with strakes than for the model without strakes.

Theoretical Comparison of Lift

A simple theory for predicting lift with vortex flow is presented in reference 6. This theory (derived from Newtonian impact theory) arrives at a second-order polynomial in α for C_L'. The quadratic term is obtained by computing the crossflow normal force using flat-plate drag. The expression for C_L' is

$$C_L' = C_{L_\alpha}'\alpha + 2\alpha^2 \tag{1}$$

where the coefficient of the linear term is obtained from reference 7. A comparison of the theoretical and experimental lift curves for the basic wing and the smaller and larger strakes is presented in figure 20.

The predicted lift is slightly below the measured values for angles of attack above about 8°, except for the basic wing for which the agreement is good up to 18° (see fig. 20(c)). The lift curves agree very well at small angles of attack; hence, the discrepancy is due to the fact that the nonlinear term of equation (1) does not completely account for the vortex lift. Figure 20(b) indicates a maximum error of 15 percent between the predicted and experimental values of lift.

Trim C_L and L/D

The C_L and L/D characteristics for trimmed level flight are presented in figures 21 and 22 for an elevon controlled aircraft with an average static margin at low lift of 4 percent and a minimum drag coefficient of 0.011. The trim characteristics for configurations with the strakes on were derived from the data shown in figures 6, 7, 8, 9, and 11. The characteristics for the basic wing were derived from the data of figure 3.

The addition of the strakes without leading-edge flaps did not significantly affect $(L/D)_{max}$. As shown on figures 21(c) and (d), deflecting the partial-span leading-edge flaps to 30° slightly reduced $(L/D)_{max}$ for the $A = 1.34$ configuration and increased $(L/D)_{max}$ for the $A = 1.46$ configuration. (This increase was about 1.0 for the configuration with the higher strake sweep.) The effect of the slot without leading-edge flaps was to reduce $(L/D)_{max}$ slightly, as shown on figure 22. Also as shown on this figure, at $\delta_n = 30^\circ$, the combined effect of opening the slot and deflecting the leading edge full span instead of partial span was to increase L/D angles of attack above 6°. This configuration (full-span nose-flap deflection and slot open) had an almost linear lift versus moment curve (fig. 10).

Take-Off Distance

Take-off distances were computed for aircraft with strakes installed, and the results are shown in figure 23. These computations were made for a 450,000 lb aircraft with a wing loading of 70 psf, which are typical of values being considered for supersonic transports. The lift and drag characteristics used in the computations were those of figure 21 to which were added a gear drag-coefficient increment of 0.012 and the ground-effect increments of C_L and C_D indicated by the data of figures 13 through 15. Changes in trim requirements due to ground effect were not considered. It is felt that for the purpose of comparing the effect of planform on take-off distance the change in trim requirement due to ground effect is not important. Additional details used in the computation are presented in reference 5 and figure 24.

The results shown in figure 23 indicate that at $T/W = 0.4$ for 10° and 12° angle of attack take-off distance was reduced about 7 percent by the use of strakes with nose flaps undeflected. These reductions were not materially affected by the strake configuration changes of the present investigation.

CONCLUDING REMARKS

The use of strakes on a delta-winged configuration was found to increase C_L significantly at high angles of attack, but to a lesser extent at angles of attack below 12°. However, this increase in C_L was accompanied by a reduction of static longitudinal stability at high angles of attack. Deflecting the leading-edge flaps on the wing outboard of the strakes improved the linearity of the pitching-moment curve.

Predictions of the lift coefficient as a function of the angle of attack using the theory of Sacks and Burnell (ref. 6) agree reasonably well with the measured values. Better agreement was obtained, however, for the basic wing than for the wings with strakes.

The configuration with strakes showed both higher increments of lift and lower increments of pitching moment due to ground proximity than the configuration without strakes.

Ames Research Center
National Aeronautics and Space Administration
Moffett Field, Calif., May 27, 1966
720-01-00-01

REFERENCES

1. Bergesen, Lt. Andrew J.; and Porter, James, D.: An Investigation of the Flow Around Slender Delta Wings with Leading Edge Separation. Rep. 510, Princeton Univ., Dept. Aero. Engr., May 1960.

2. Marsden, D. J.; Simpson, R. W.; and Rainbird, W. J.: The Flow Over Delta Wings at Low Speeds with Leading Edge Separation. Rep. 114, The College of Aeronautics, Cranfield, Gt. Brit., Feb. 1958.

3. Barlett, G. E.; and Vidal, R. J.: Experimental Investigation of Influence of Edge Shape on the Aerodynamic Characteristics of Low Aspect Ratio Wings at Low Speeds. J. Aero. Sci., vol. 22, Aug. 1955, pp. 517-533.

4. Anon.: Analysis of Longitudinal Aerodynamic Characteristics of the .0075 Scale and the .03 Scale Supersonic Transport Model at Mach Numbers of .23 to 3.06. NA-64-13, North American Aviation, Inc., Engineering Dept. Aerothermo Design, SST Project, 3 January 1964.

5. Koenig, David G.; and Corsiglia, Victor R.: Large-Scale Wind-Tunnel Tests on an Aspect Ratio 2.17 Delta Wing Model Equipped With Midchord Boundary-Layer Control Flaps. NASA TN D-2552, 1964.

6. Sacks, Alvin H.; and Burnell, Jack A.: On the Use of Impact Theory for Slender Configurations Exhibiting Flow Separation. Vidya 92, Itek Corp., 31 March 1963.

7. De Young, John; and Harper, Charles W.: Theoretical Symmetric Span Loading at Subsonic Speeds for Wings Having Arbitrary Planform. NACA Rep. 921, 1948.

TABLE I.- PLANFORM CHARACTERISTICS

A	Λ_s	S', sq ft	η_{IB}	$\bar{c}$, ft	λ	b	Tip
1.46	73	505	0.484	24.1	0.091	27.3	Off
1.34	73	556	.628	27.2	.083	↓	↓
1.34	77	555	.473	28.3	.075		
1.46	77	512	.379	25.4	.082		
1.69	Basic wing	439	---	19.4	.123		

TABLE II.- LIST OF FIGURES

Figure	Configuration	δ_{n_s}, deg	δ_n, deg	δ_f, deg	$h/\bar{c}$	Comments
3(a)	Basic wing		0	0, 10 0	∞	Tips off Tips on
3(b)			30, 45	0, 10		Tips on
4	$\Lambda_s = 73^\circ$, A = 1.46, 1.34	0	0	0		Tips on, off
5(a)	$\Lambda_s = 77^\circ$, A = 1.46, 1.34		0	0		Tips on, off
5(b)			30			
6(a)	$\Lambda_s = 77^\circ$, A = 1.34		0	-5, 0, 10		
6(b)			30			
7(a)	$\Lambda_s = 73^\circ$, A = 1.34		0	-5, 0, 10		
7(b)			30			
8(a)	$\Lambda_s = 77^\circ$, A = 1.46		0	-5, 0, 10		
8(b)			30			
9(a)	$\Lambda_s = 73^\circ$, A = 1.46		0	-5, 0, 10		
9(b)			30			
10(a)	$\Lambda_s = 77^\circ$, A = 1.46	30	0, 30	0		Slot open, closed and full span L.E. flap
11(a)	$\Lambda_s = 77^\circ$, A = 1.46	0	0	-5, 0, 10		Slot open
11(b)			30			Slot open and full span L.E. flap
12(a)	$\Lambda_s = 77^\circ$, A = 1.34		0	0		Slots A, B, C, and L.E. notch
13	Basic wing		0	0	Variable	
14(a)	$\Lambda_s = 77^\circ$, A = 1.46		0	0	Variable	
15(a)	$\Lambda_s = 77^\circ$, A = 1.34		0	0	Variable	
16(a)	$\Lambda_s = 77^\circ, 73^\circ$, A = 1.46, 1.34		0	0	∞	C_L vs. α only
16(b)			30			
17	$\Lambda_s = 77^\circ$, A = 1.46		0	0	Variable	C_L vs. $h/\bar{c}$
18(a)	$\Lambda_s = 77^\circ, 73^\circ$, A = 1.46, 1.34		0	0	∞	C_L vs. C_m only
18(b)			30			
19	$\Lambda_s = 77^\circ$, A = 1.46		0	0	Variable	C_m vs. $h/\bar{c}$
20(a) 20(b) 20(c)	A = 1.34 A = 1.46 Basic wing (A = 1.69)		0	0	∞	Theory comparison. The reference area includes the strake area. See table II.
21(a) 21(b) 21(c) 21(d)	$\Lambda_s = 73^\circ$, A = 1.46, 1.34 $\Lambda_s = 77^\circ$, A = 1.46, 1.34 $\Lambda_s = 77^\circ, 73^\circ$, A = 1.34 $\Lambda_s = 77^\circ, 73^\circ$, A = 1.46		0 0, 30 0, 30	0		$C_{L_{trim}}$ = L/D_{trim} and α
22	$\Lambda_s = 77^\circ$, A = 1.46	30	0, 30			Slot open, full span L.E. flap
23	A = 1.34, 1.46, 1.69	0	0, 30			Take-off distance vs. T/W
24						Engine characteristics for figure 23

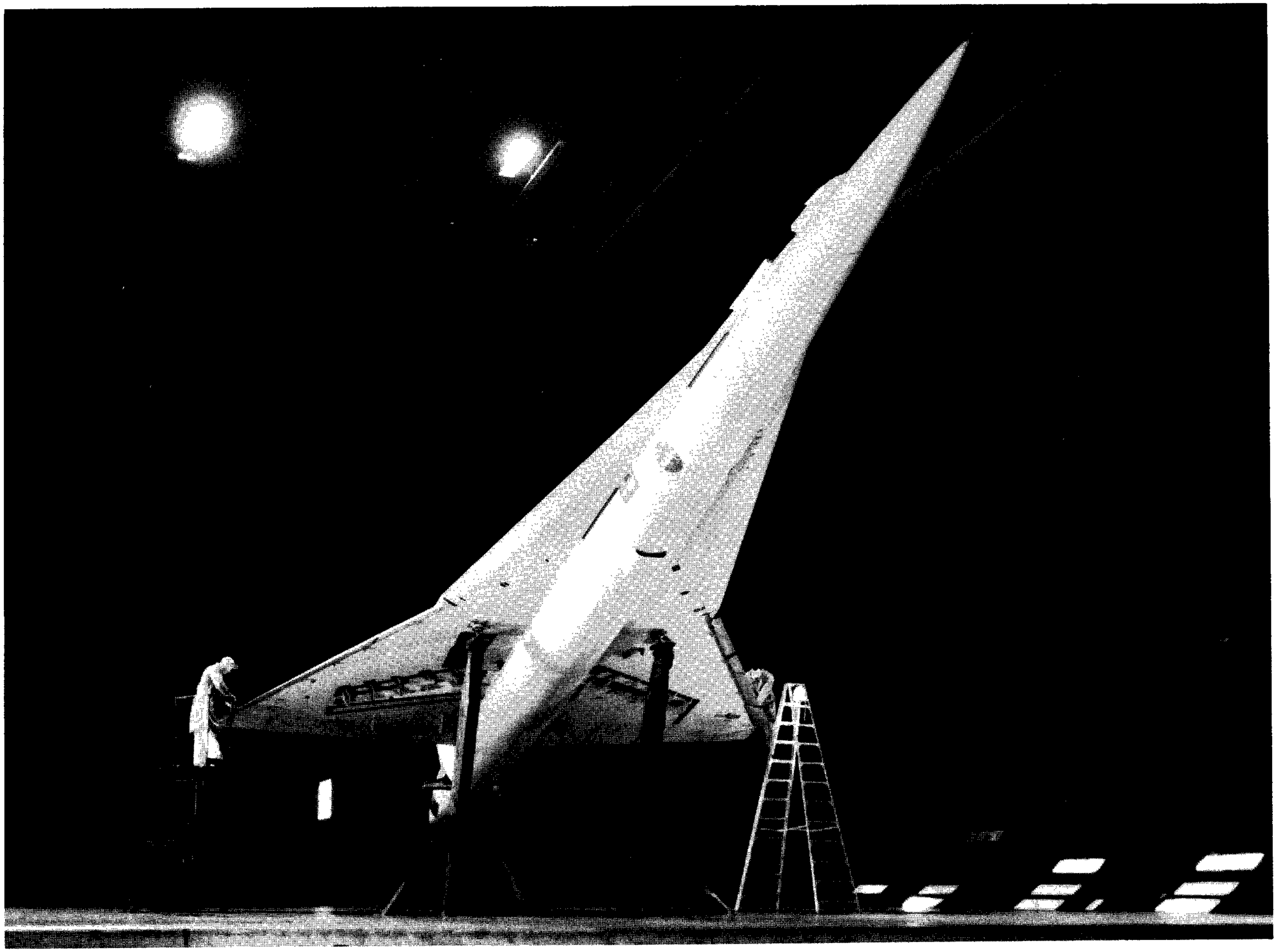

A-31802

Figure 1.- The model shown mounted in the Ames 40- by 80-Foot Wind Tunnel.

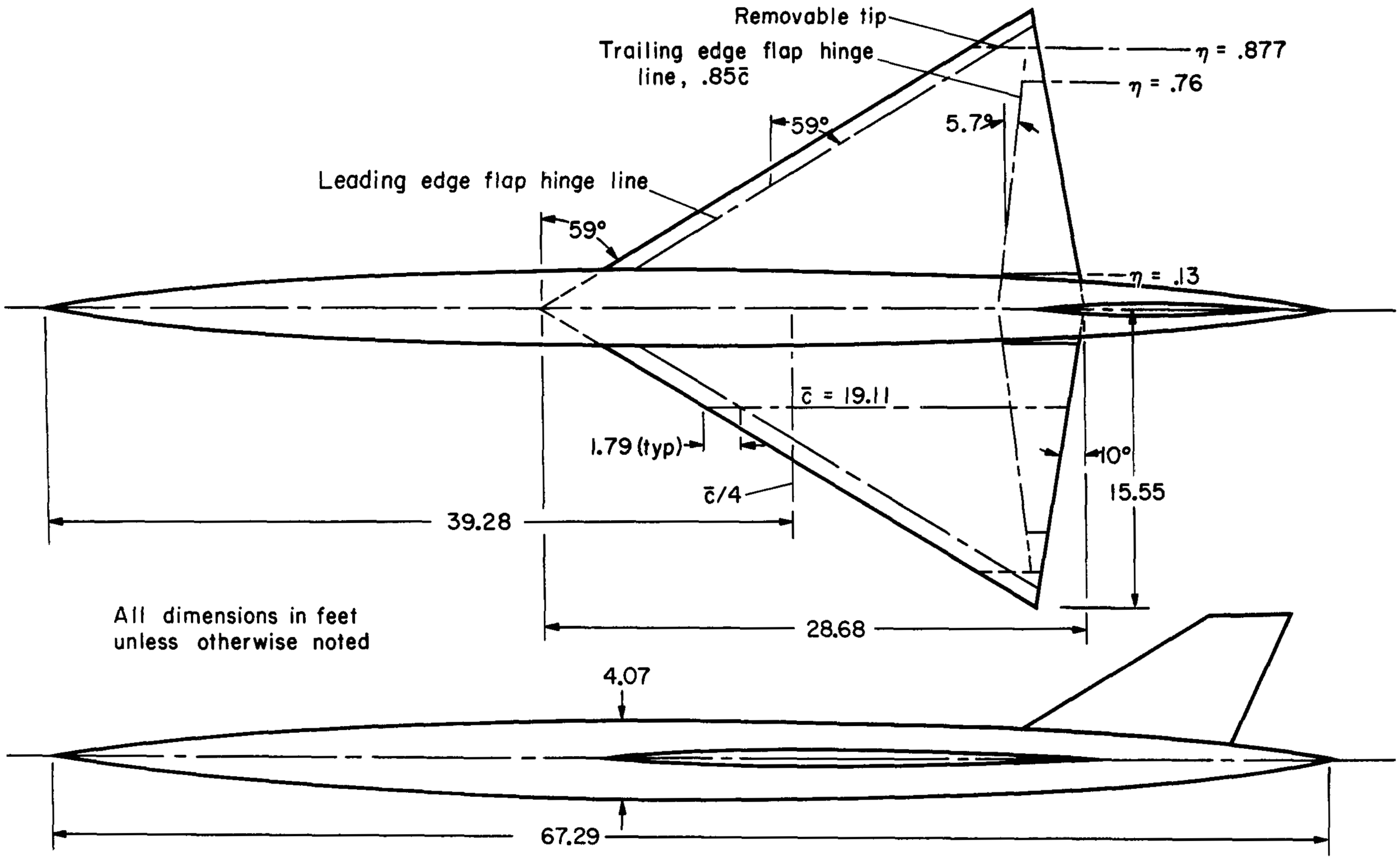

(a) Two views of the model.

Figure 2.- Geometric details of the model without strakes.

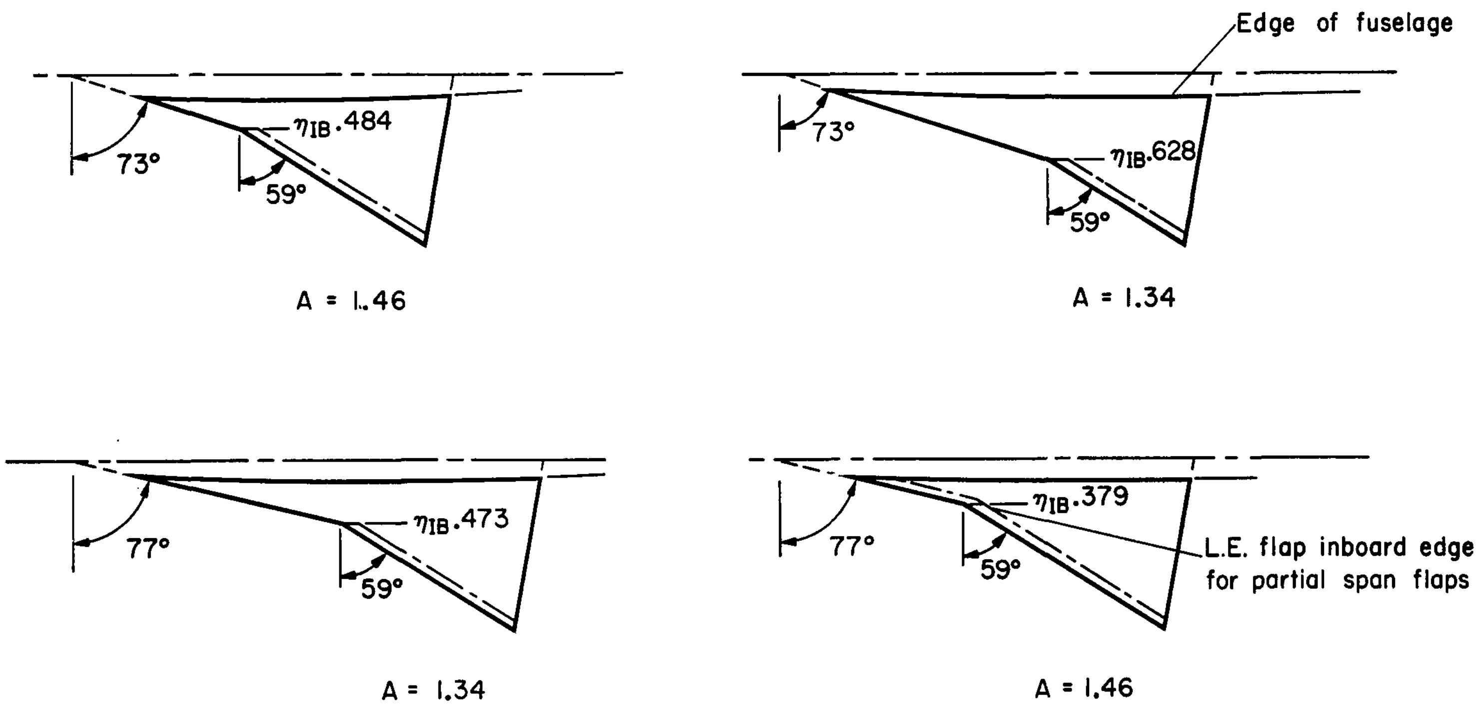

(b) Planforms tested with strakes.

Figure 2.- Continued.

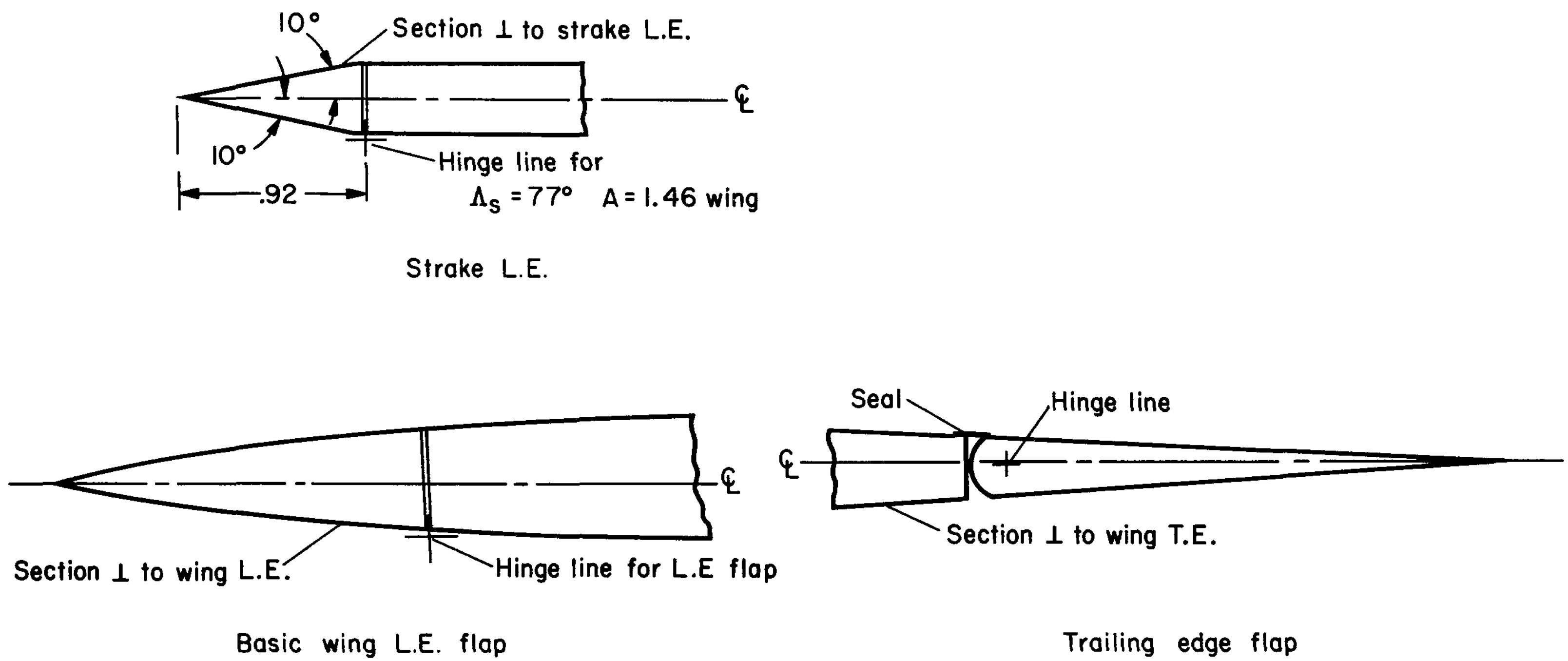

(c) Details of the leading-edge contour and of the hinge-line location.

Figure 2.- Continued.

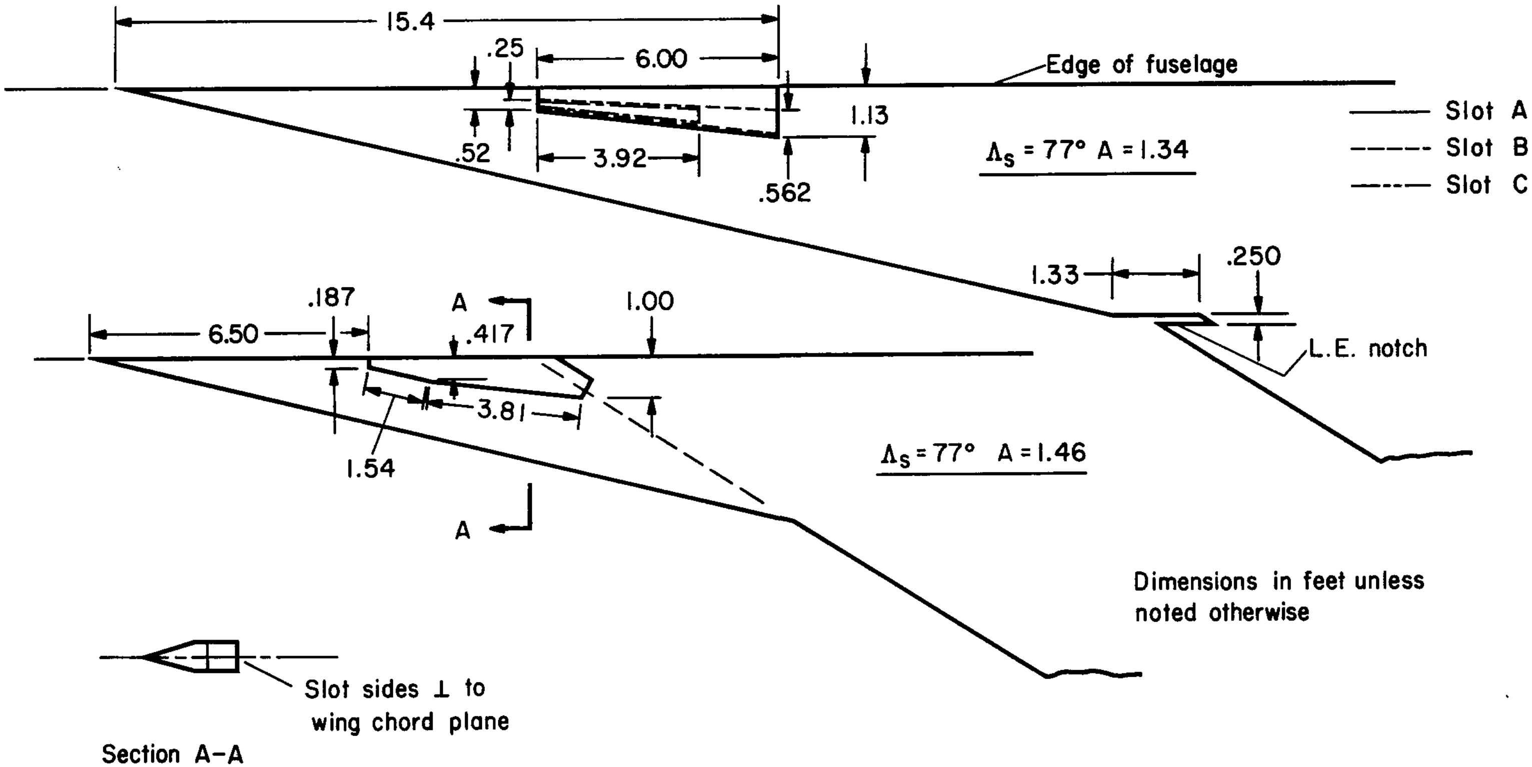

(d) Details of the slot configurations.

Figure 2.- Concluded.

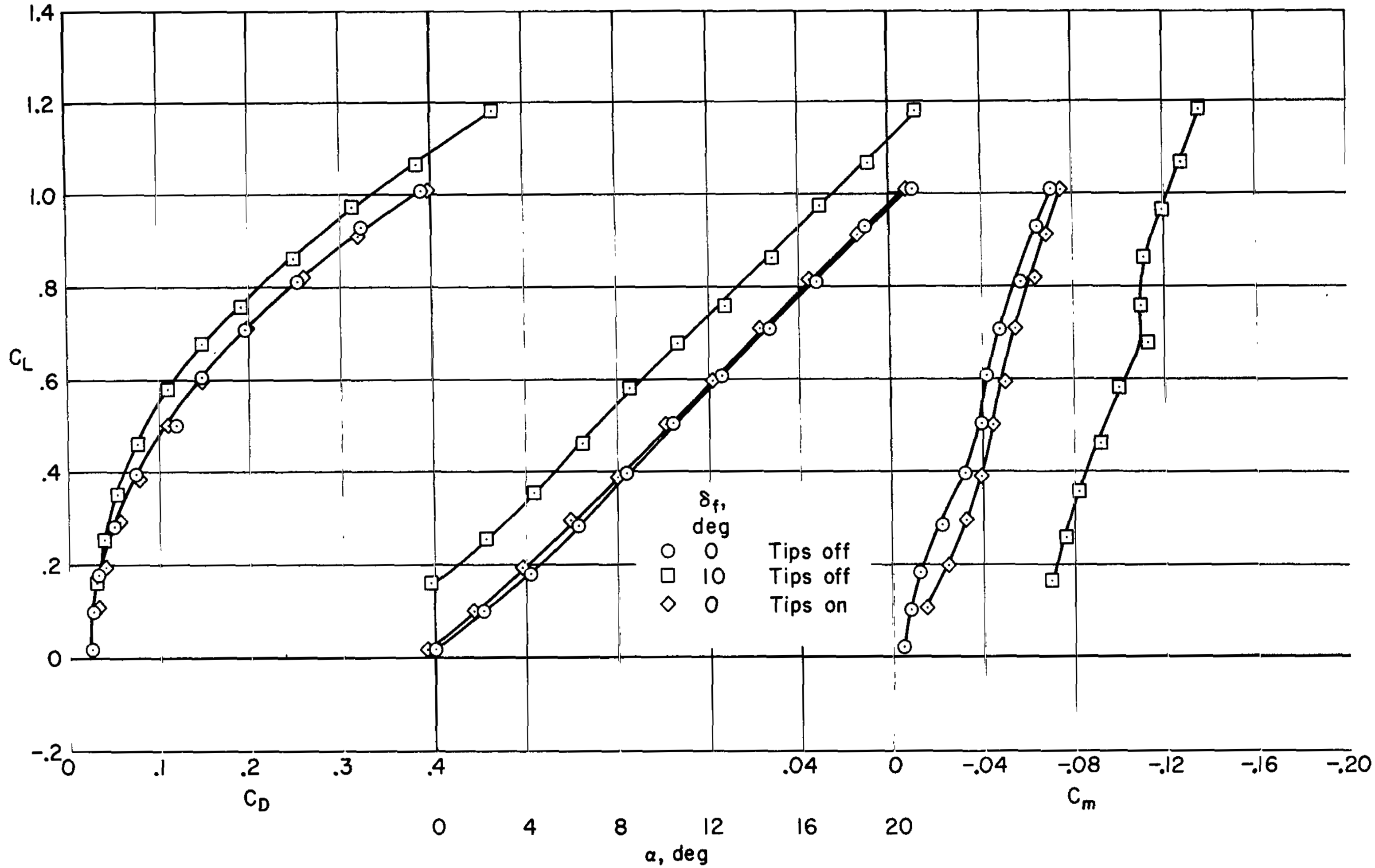

(a) $\delta_n = 0^{\circ}$

Figure 3.- The characteristics of the model without strakes; $h/\overline{c} \to \infty$.

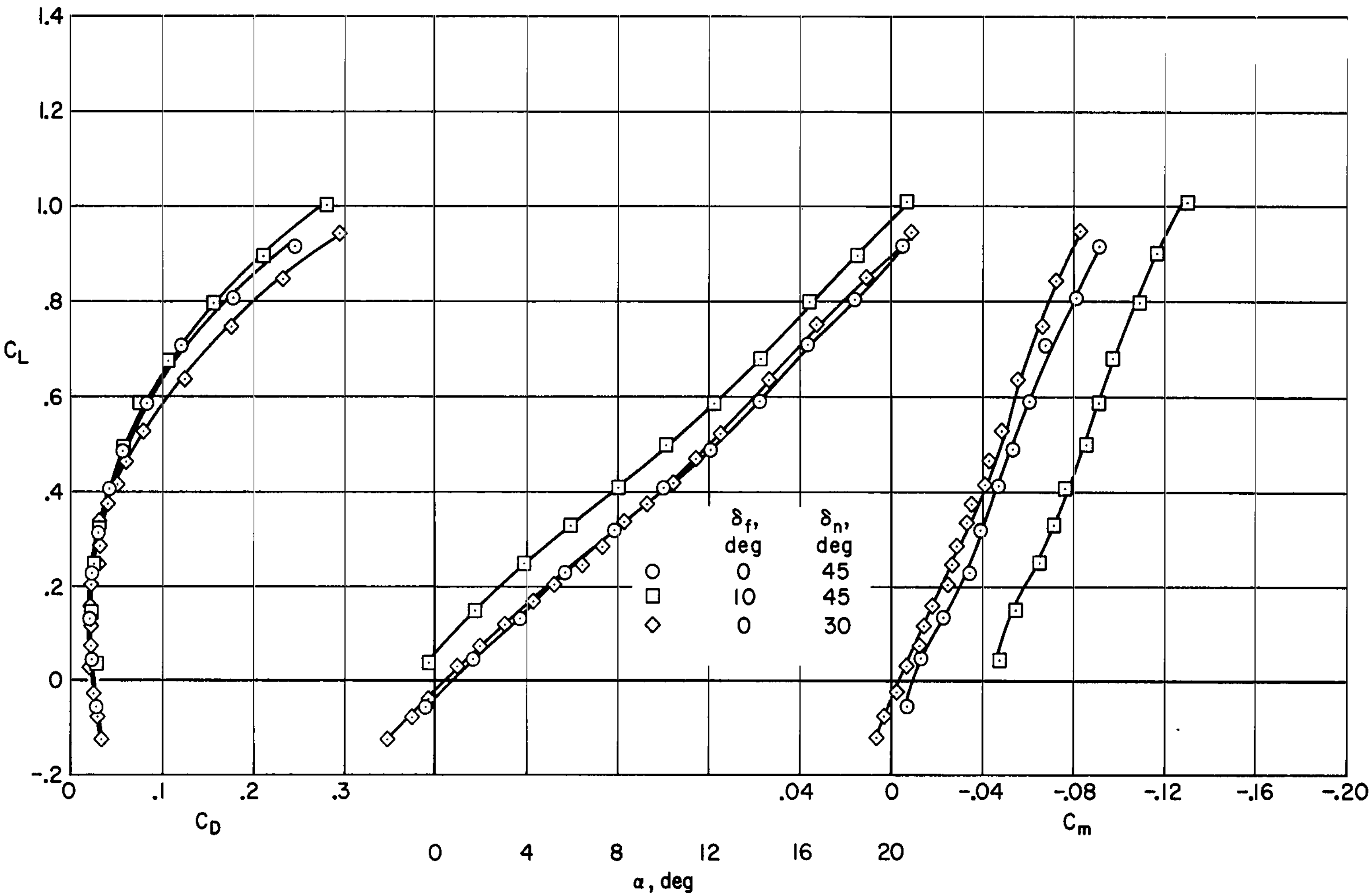

(b) Wing tips on.

Figure 3.- Concluded.

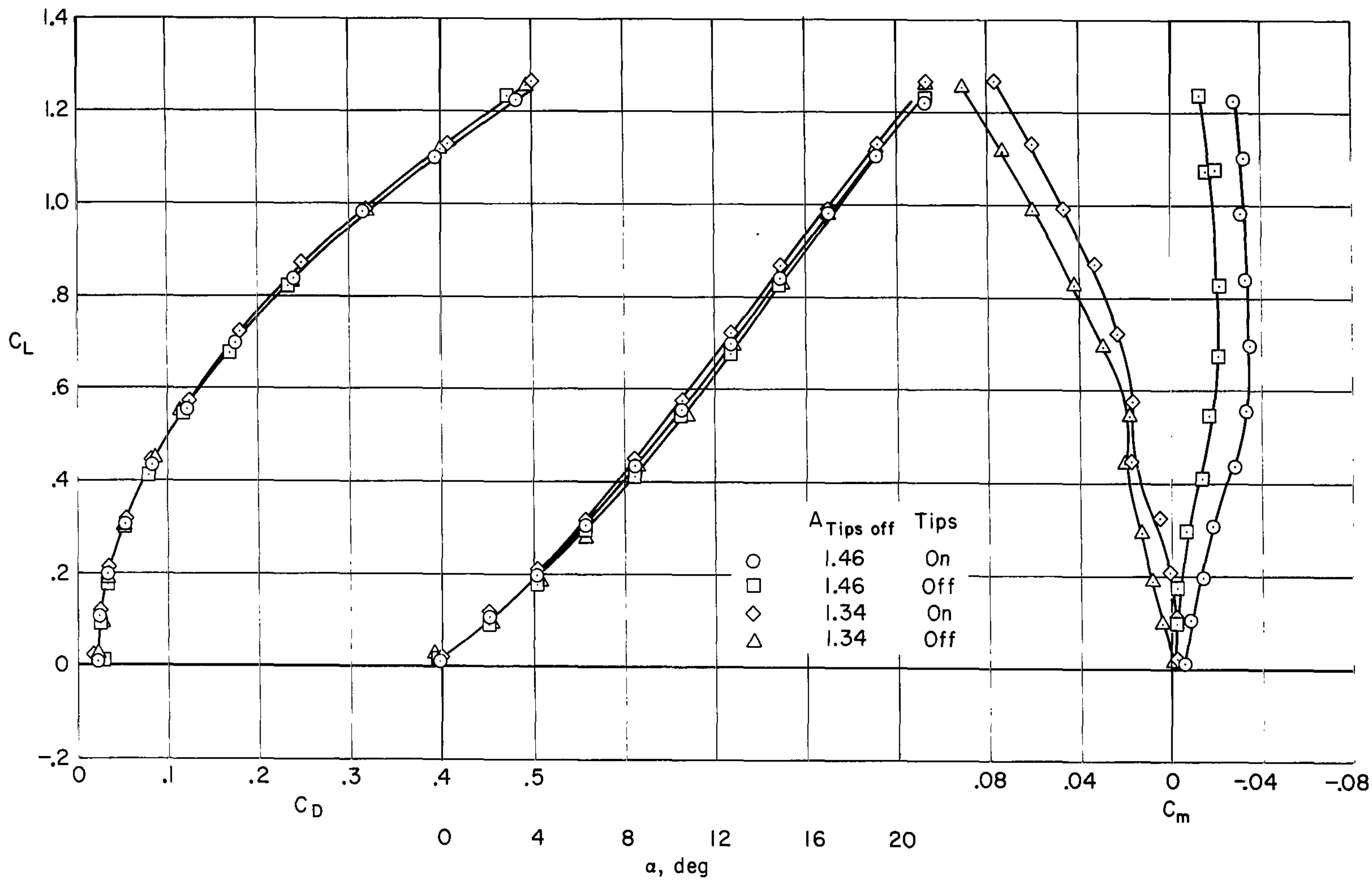

Figure 4.- The effect of wing tips with the 73° strakes; $\delta_n = 0^{\circ}$, $\delta_f = 0^{\circ}$, $h/\bar{c} \rightarrow \infty$.

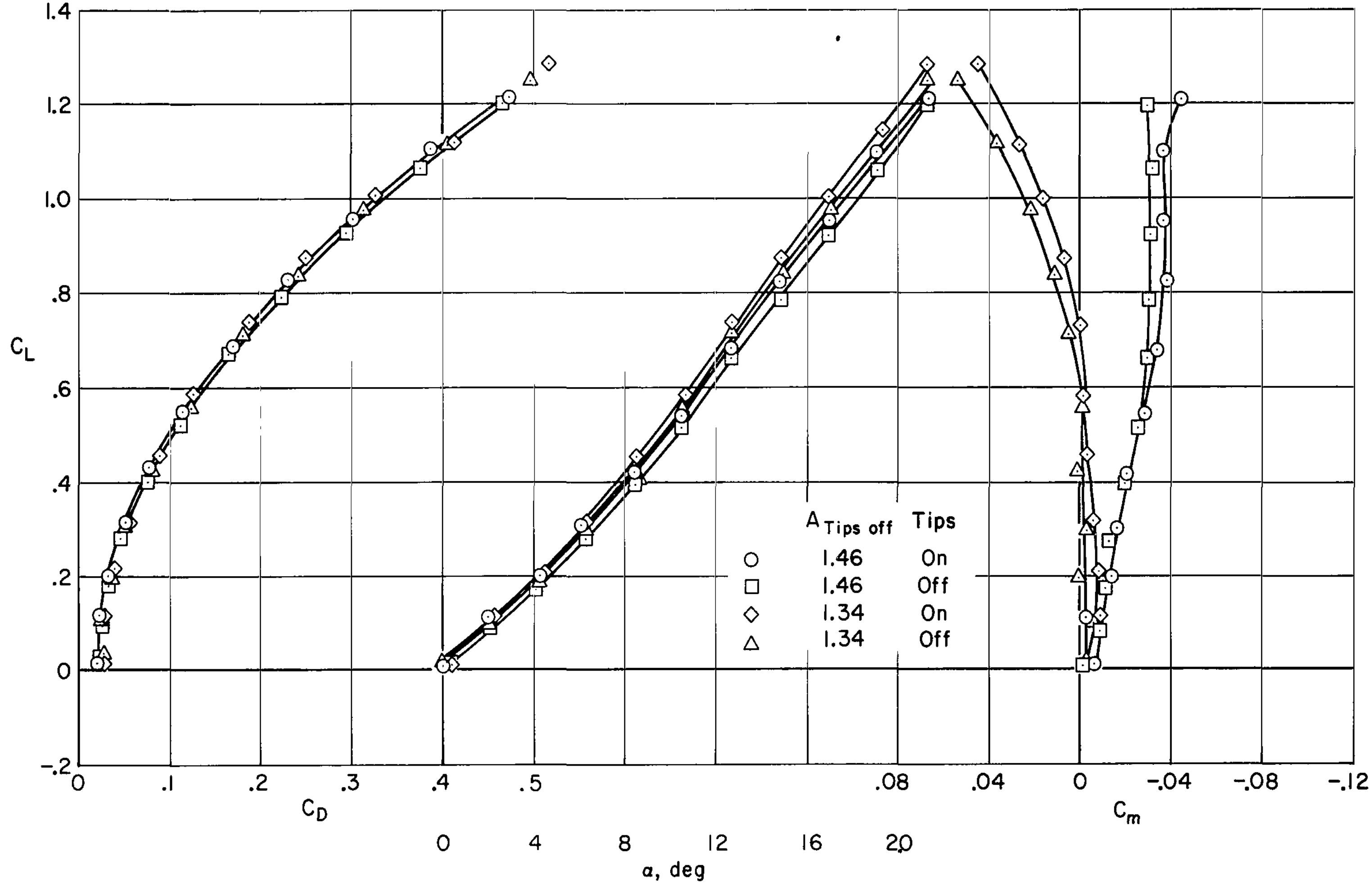

(a) $\delta_n = 0^{\circ}$

Figure 5.- The effect of wing tips with the 77° strakes; $\delta_f = 0^{\circ}$, $h/\bar{c} \rightarrow \infty$.

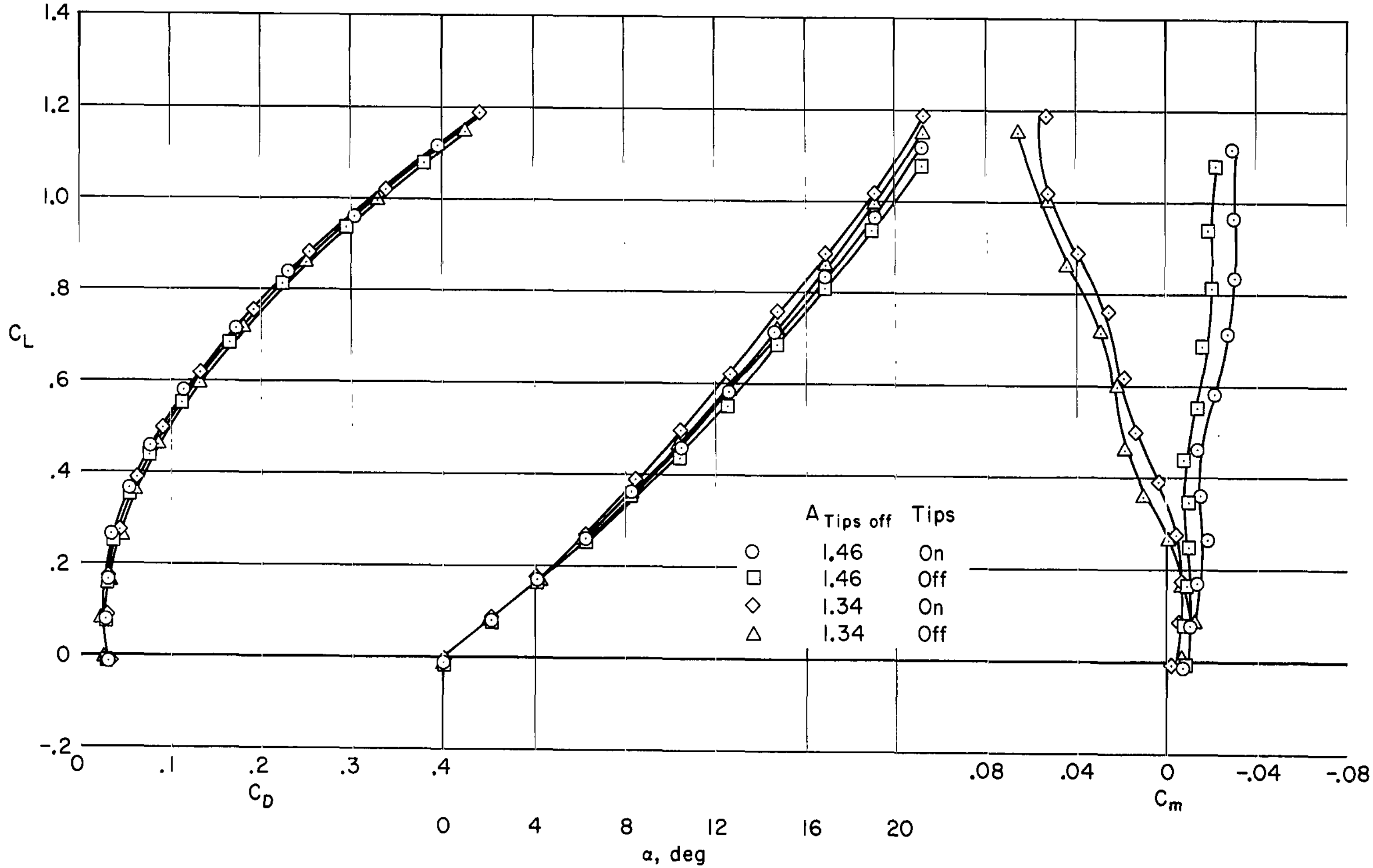

(b) $\delta_n = 30^\circ$; partial span.

Figure 5.- Concluded.

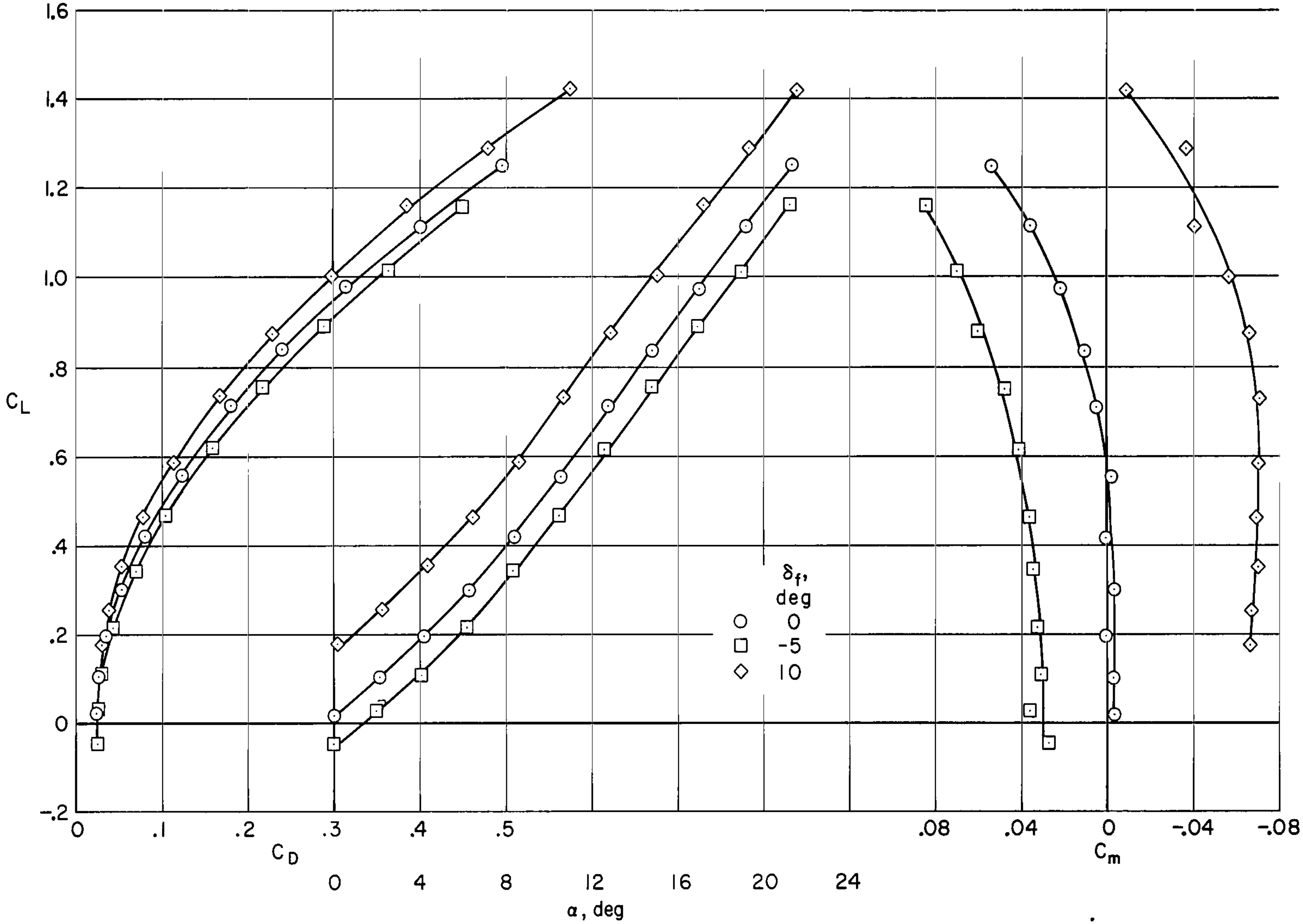

(a) $\delta_n = 0^{\circ}$

Figure 6.- The characteristics of the model with the larger 77° strakes; $A = 1.34$, tips off, $h/\bar{c} \rightarrow \infty$.

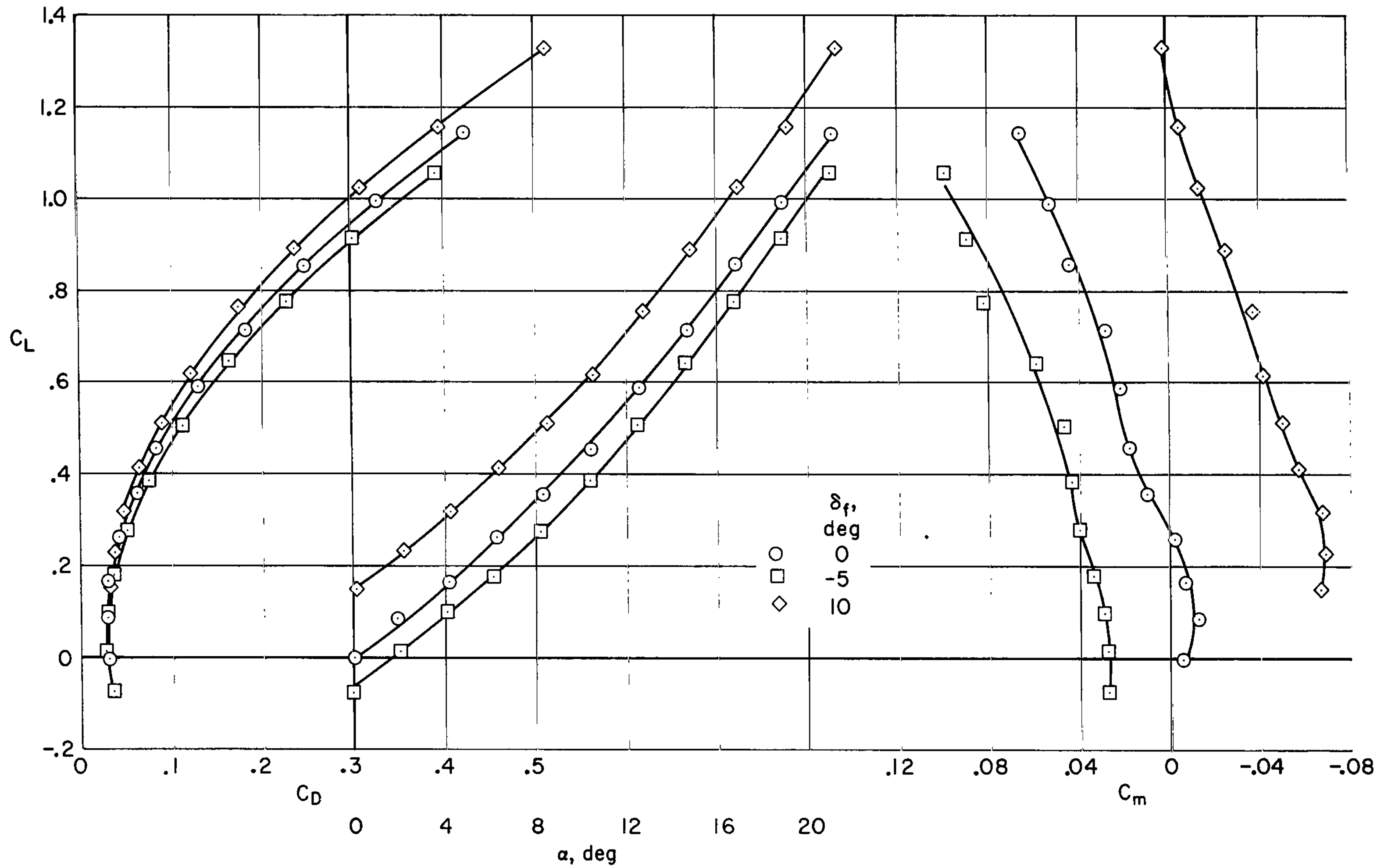

(b) $\delta_n = 30^{\circ}$; partial span.

Figure 6.- Concluded.

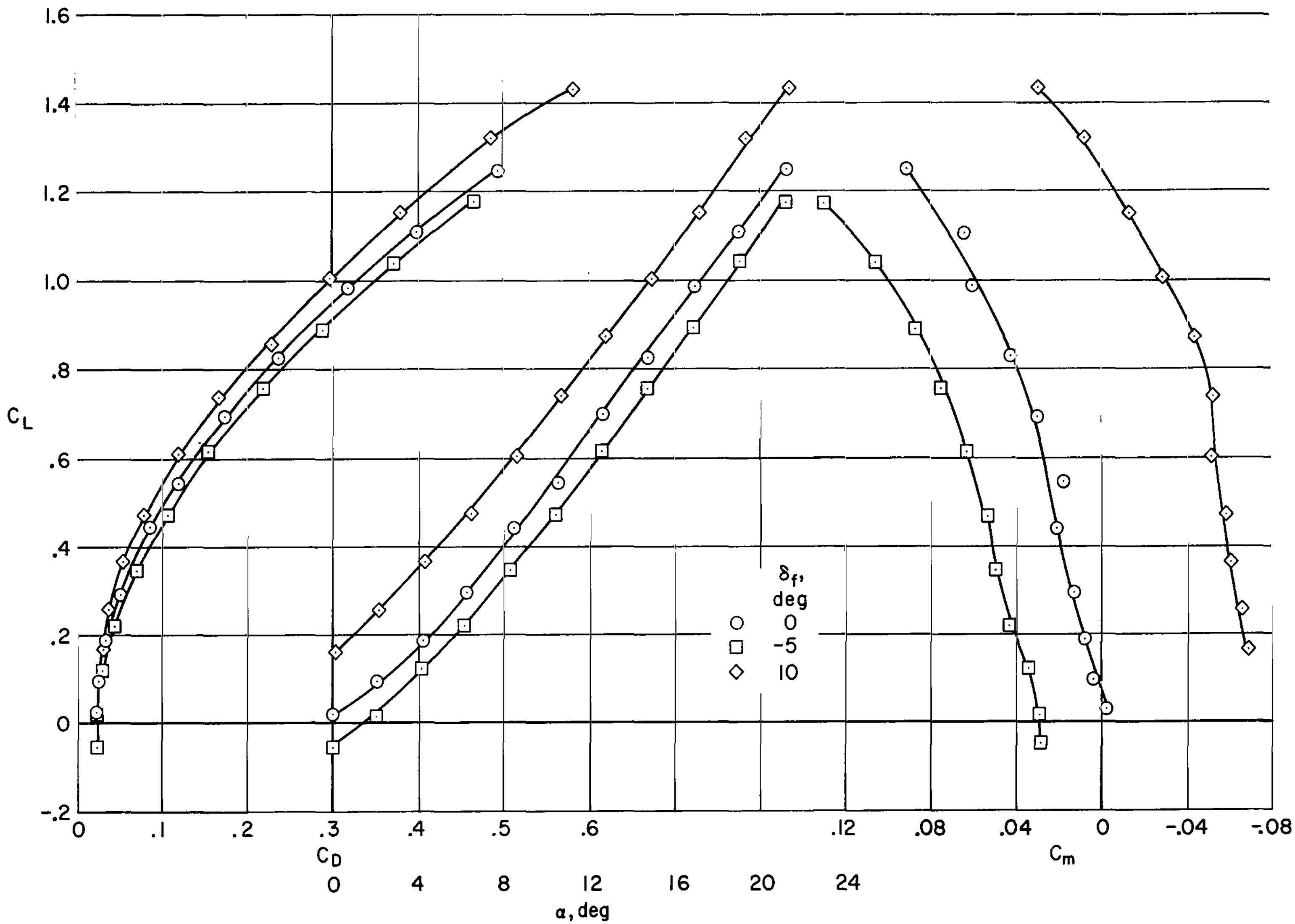

(a) $\delta_n = 0^{\circ}$

Figure 7.- The characteristics of the model with the larger 73° strakes; A = 1.34, tips off, $h/\bar{c} \rightarrow \infty$.

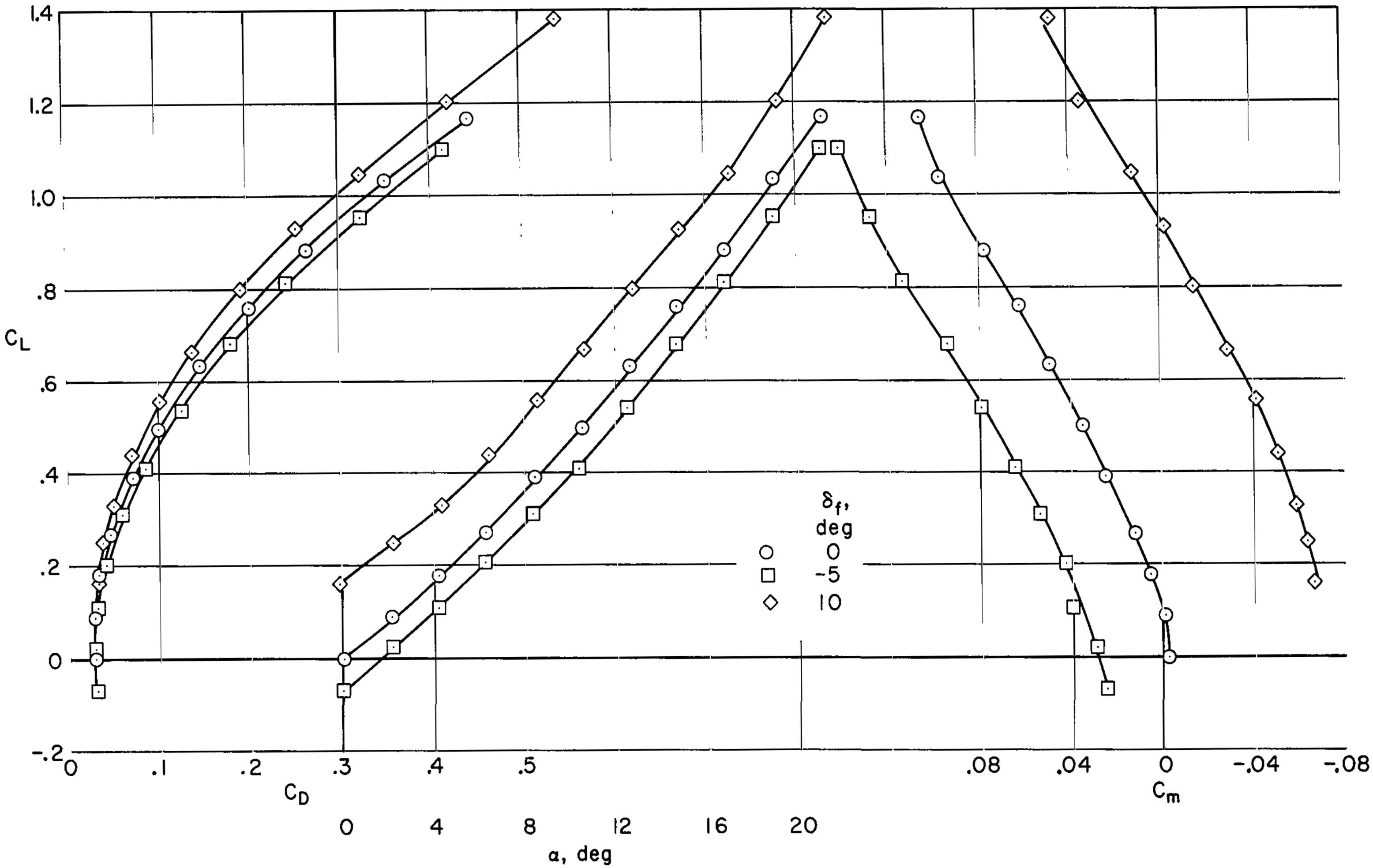

(b) $\delta_n = 30^{\circ}$, partial span.

Figure 7.- Concluded.

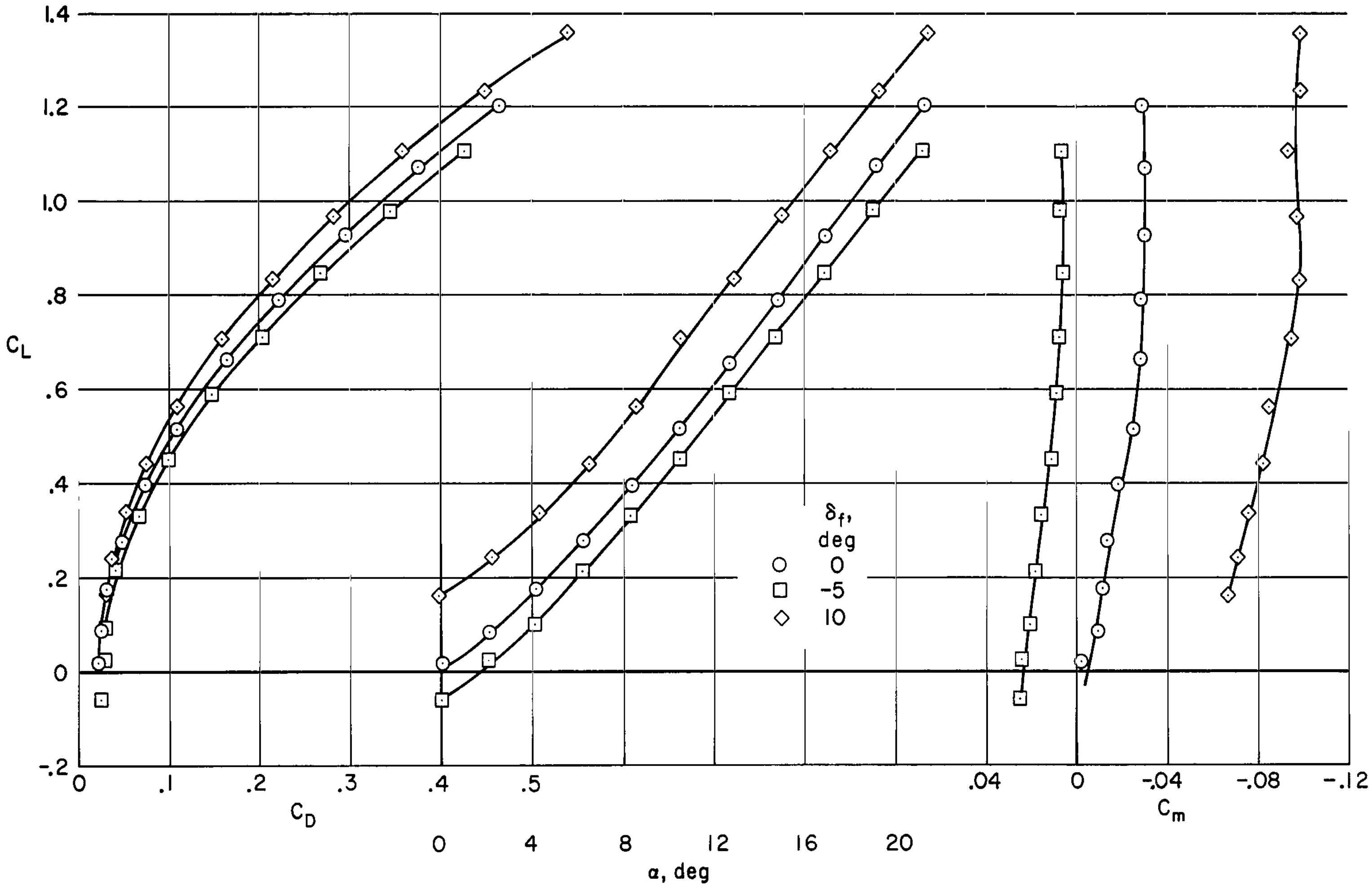

(a) $\delta_n = 0^{\circ}$

Figure 8.- The characteristics of the model with the smaller 77° strakes; $A = 1.46$, tips off, $h/\bar{c} \rightarrow \infty$.

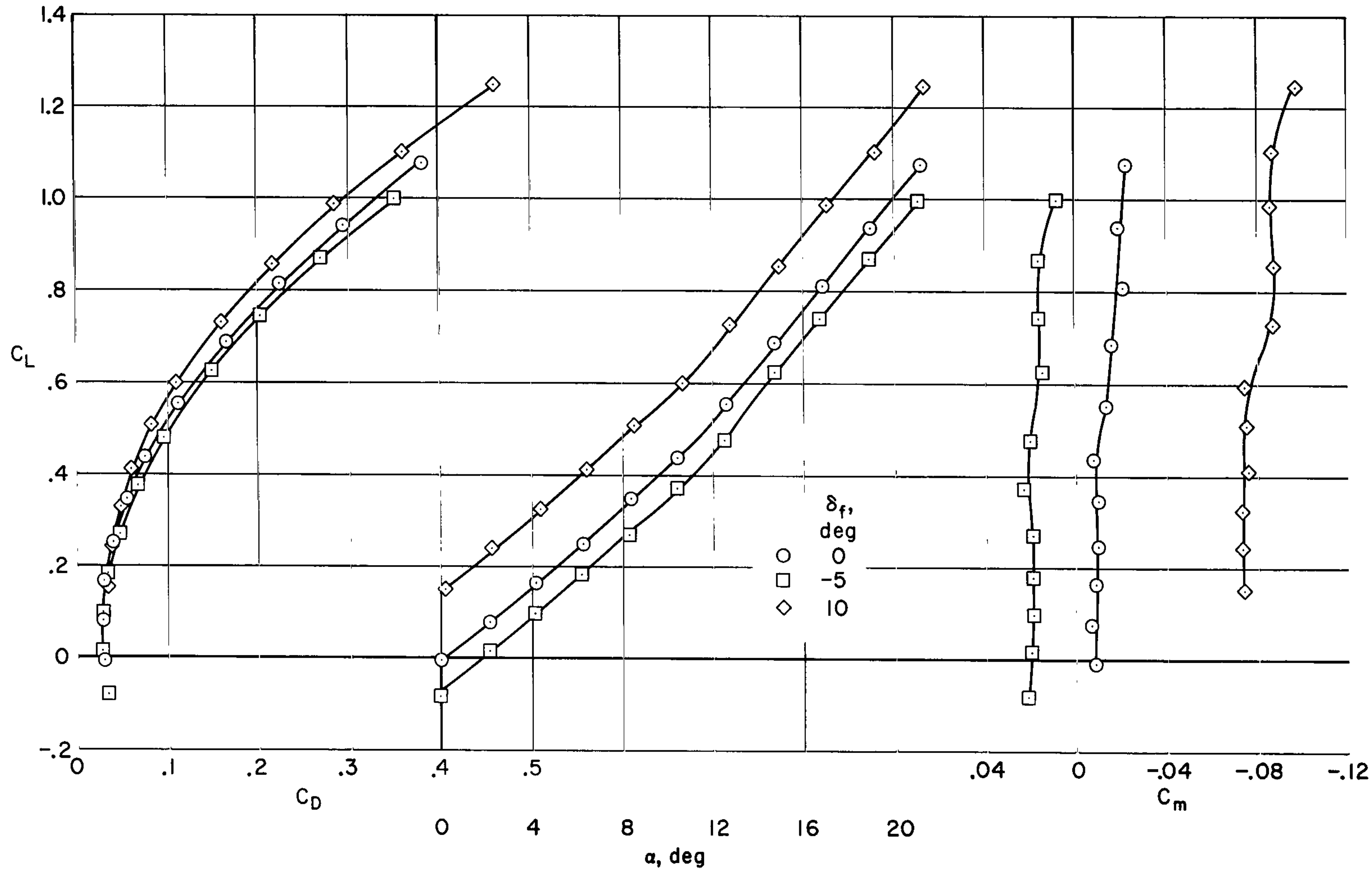

(b) $\delta_n = 30^{\circ}$, partial span.

Figure 8.- Concluded.

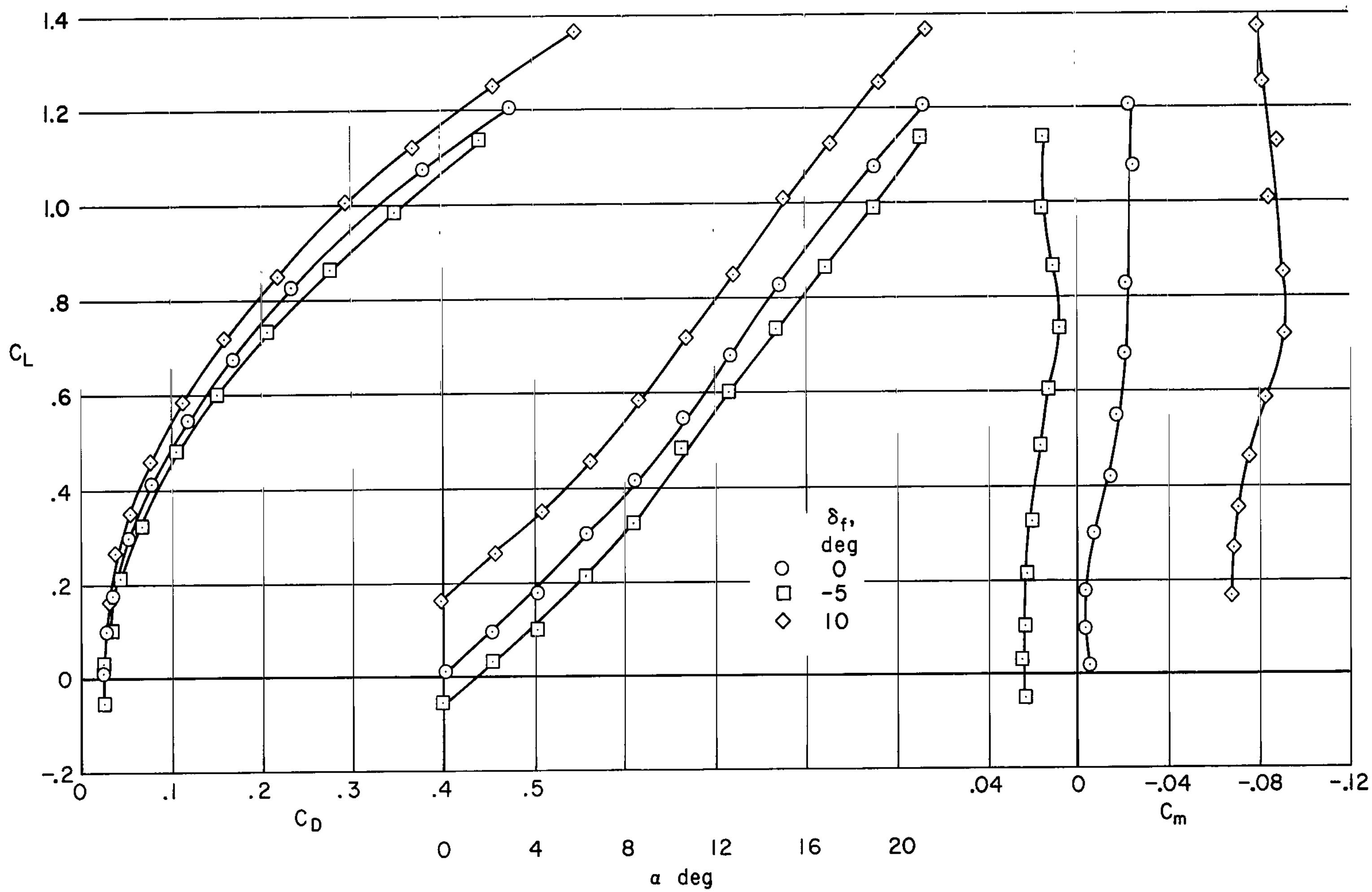

(a) $\delta_n = 0^\circ$

Figure 9.- The characteristics of the model with the smaller 73° strakes; $A = 1.46$, tips off, $h/\bar{c} \rightarrow \infty$.

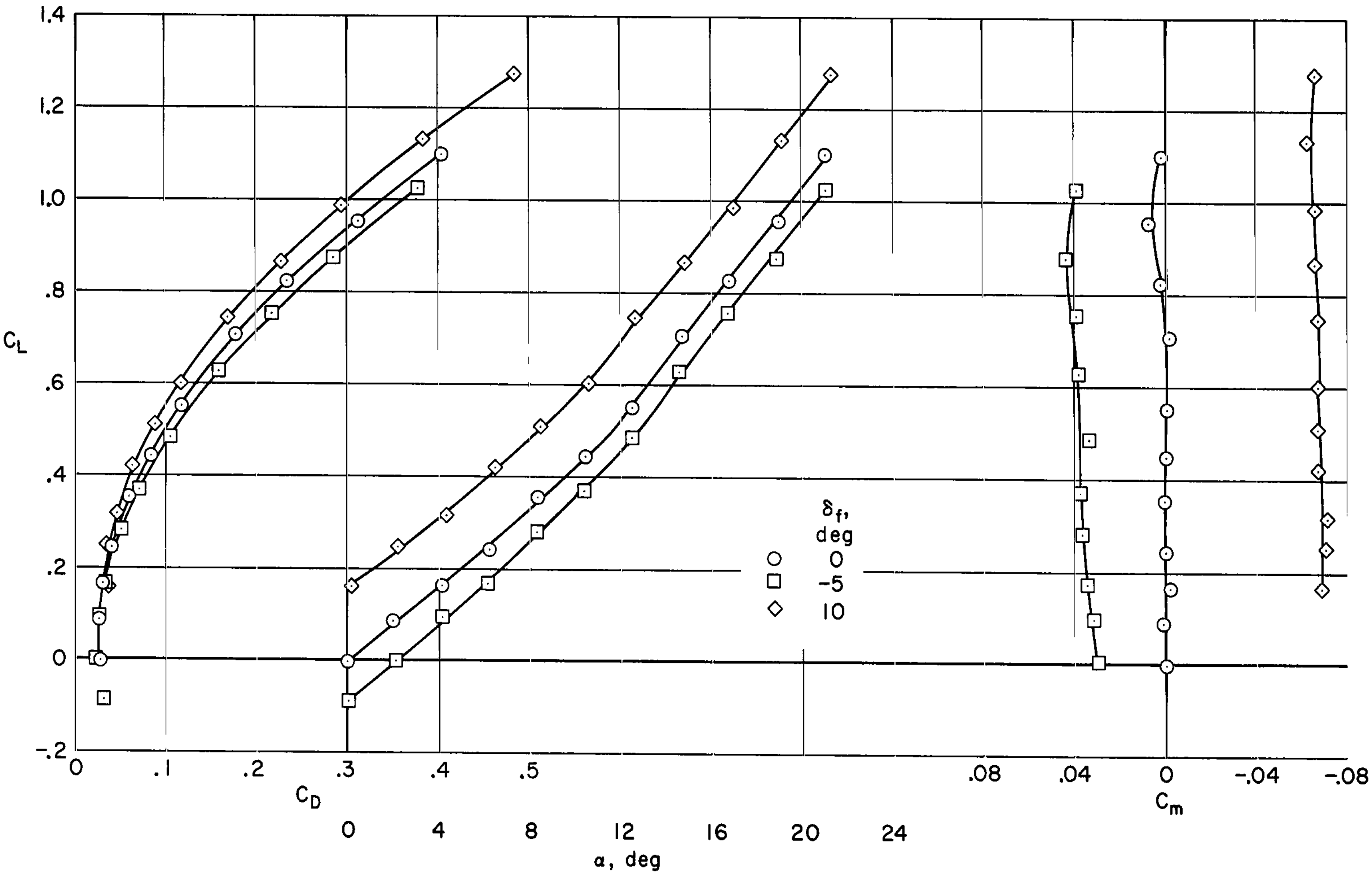

(b) $\delta_n = 30^\circ$, partial span.

Figure 9.- Concluded.

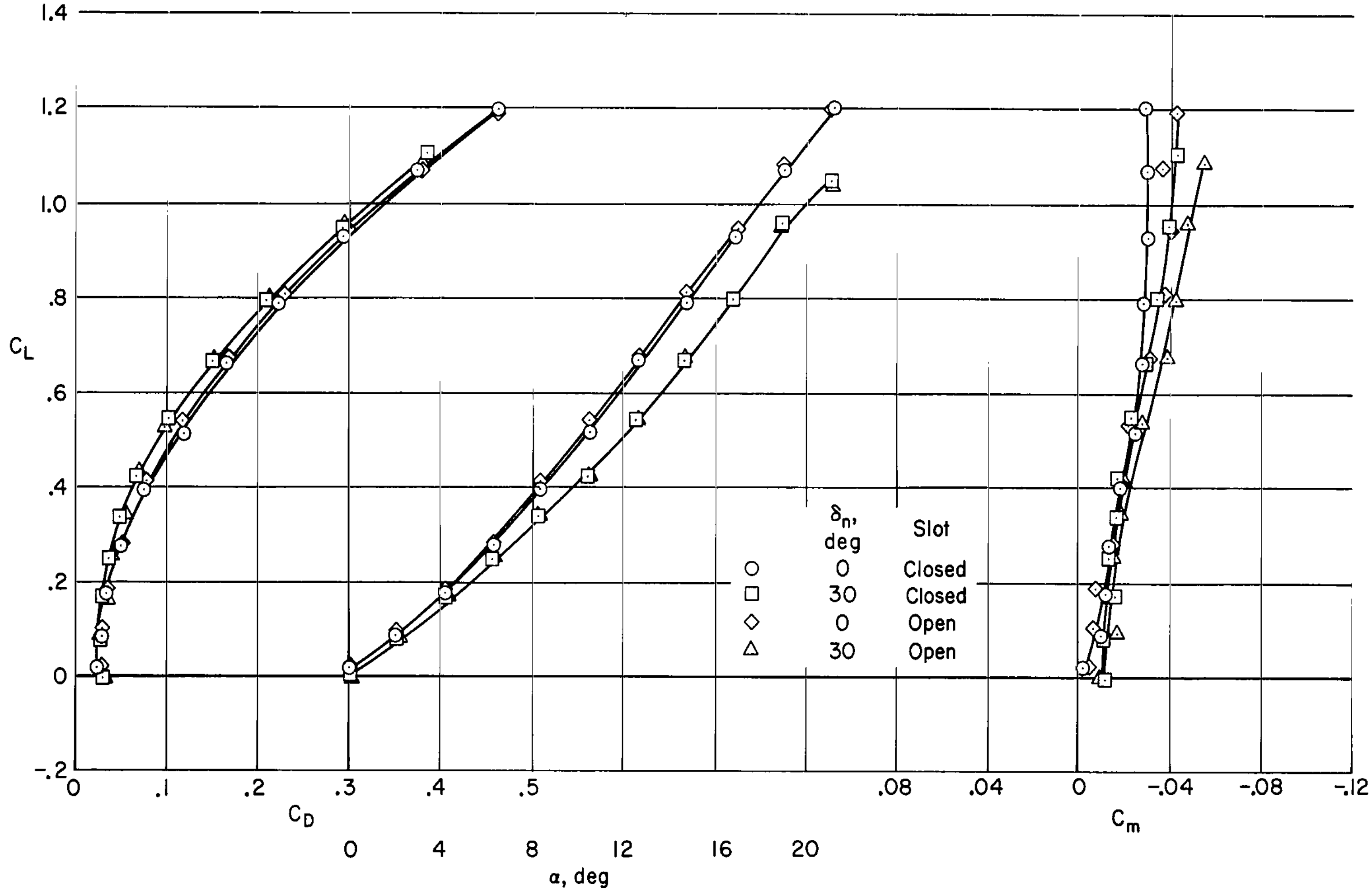

Figure 10.- The effect of opening the slot in the smaller 77° strake and deflecting full span leading-edge flap; $A = 1.46$, tips off, $h/\bar{c} \rightarrow \infty$.

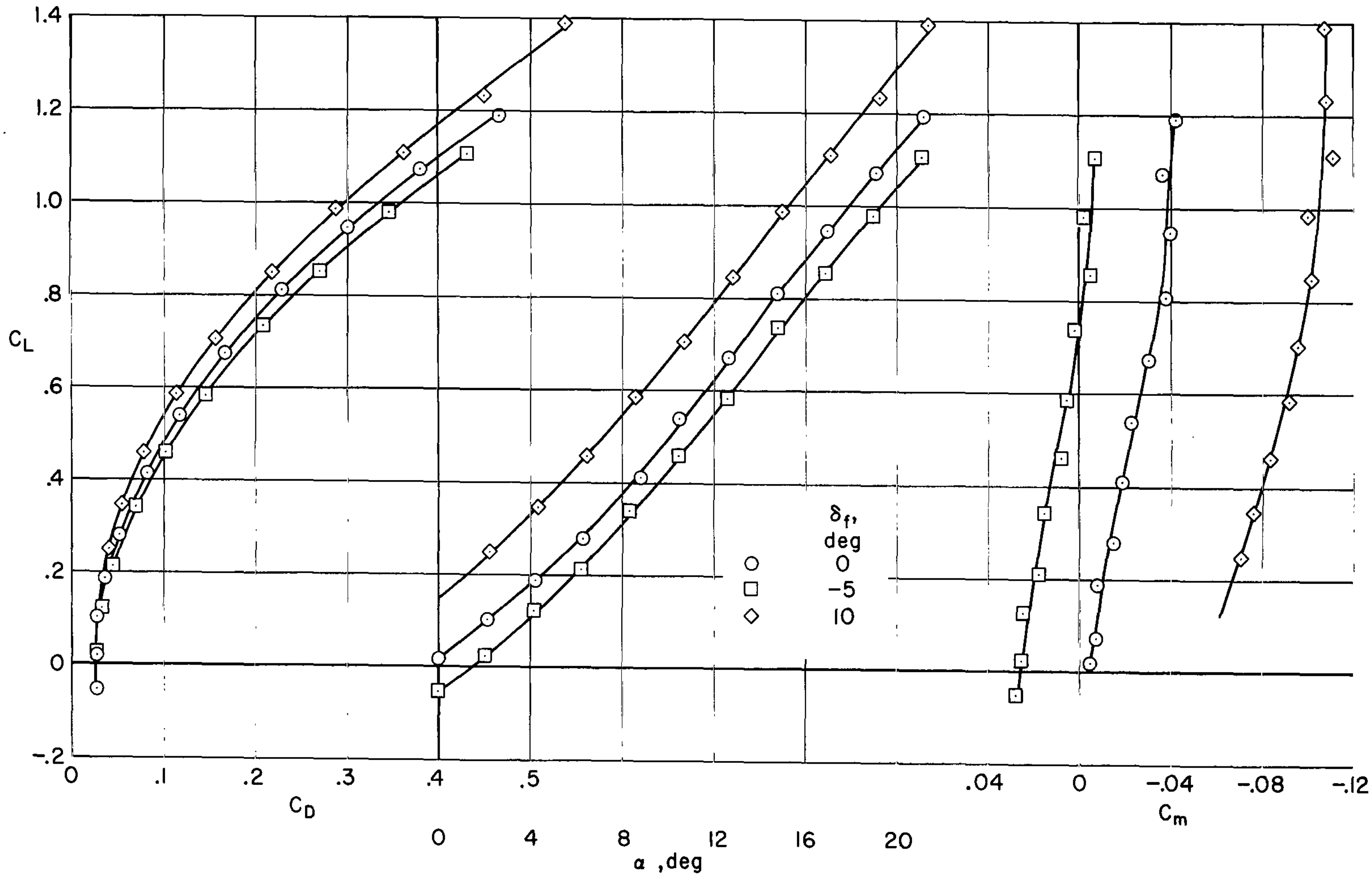

(a) $\delta_n = 0^{\circ}$

Figure 11.- The characteristics of the model with a slot in the smaller 77° strake; A = 1.46, tips off, $h/\bar{c} \rightarrow \infty$.

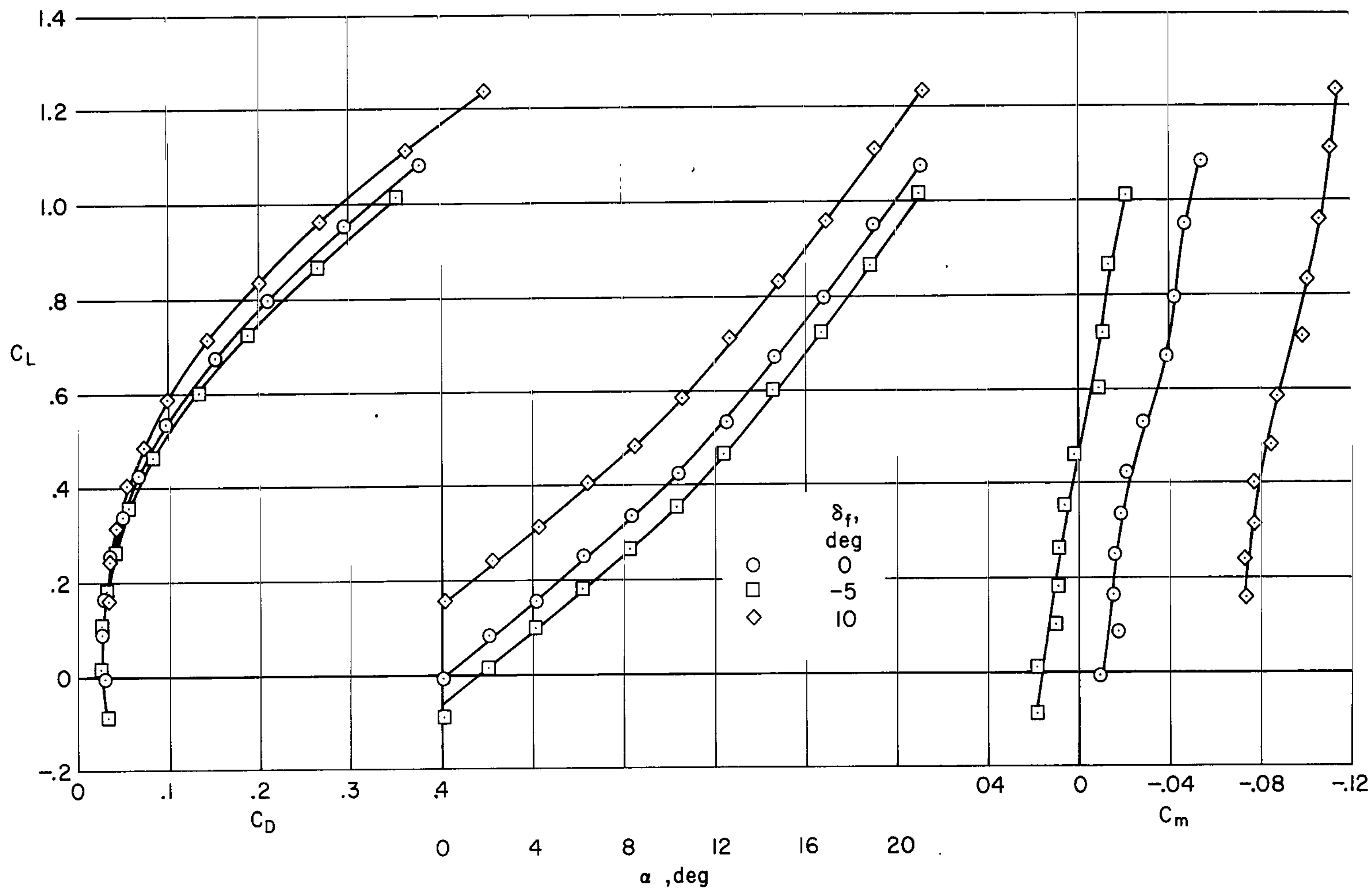

(b) $\delta_n = 30^{\circ}$, full span.

Figure 11.- Concluded.

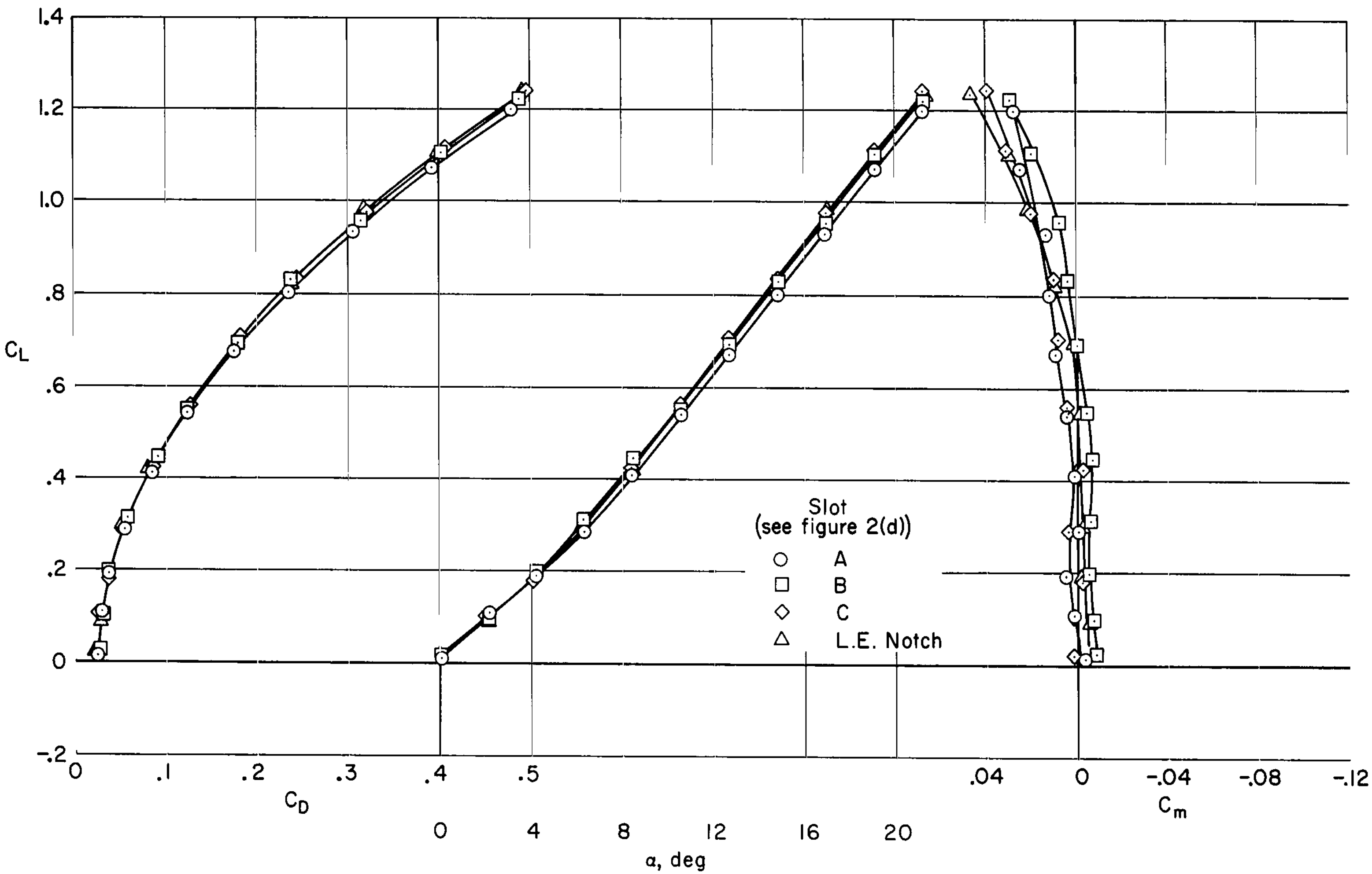

Figure 12.- The effect of slots in the larger 77° strake; $A = 1.34$, $\delta_n = 0^\circ$, $\delta_f = 0^\circ$, $h/\bar{c} \to \infty$, tips off.

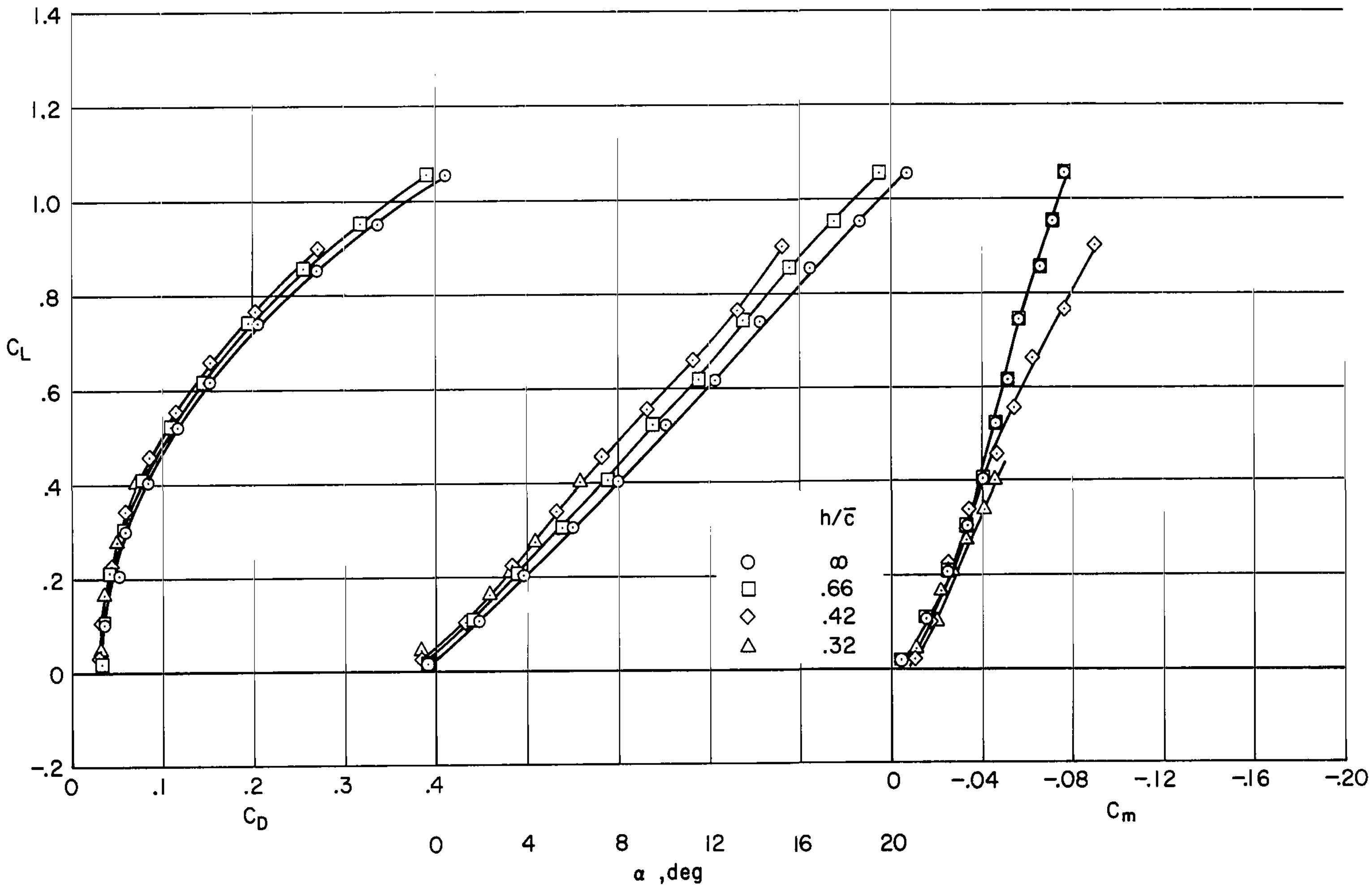

Figure 13.- The effect of ground proximity on the model without the strakes; $\delta_n = 0^o$, $\delta_f = 0^o$, tips on.

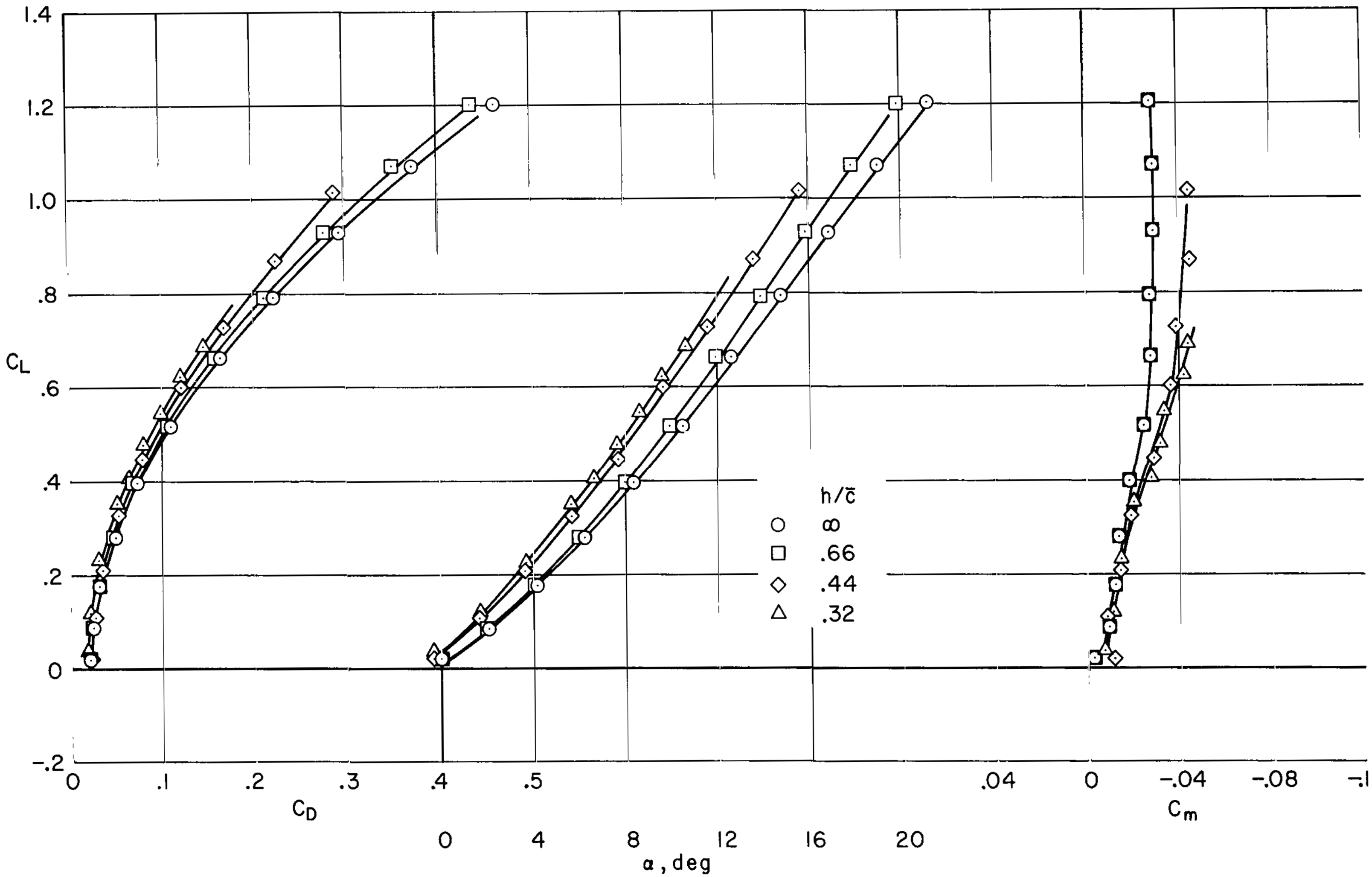

Figure 14.- The effect of ground proximity on the model with the smaller 77° strakes; A = 1.46, tips off, $\delta_n = 0^\circ$, $\delta_f = 0^\circ$.

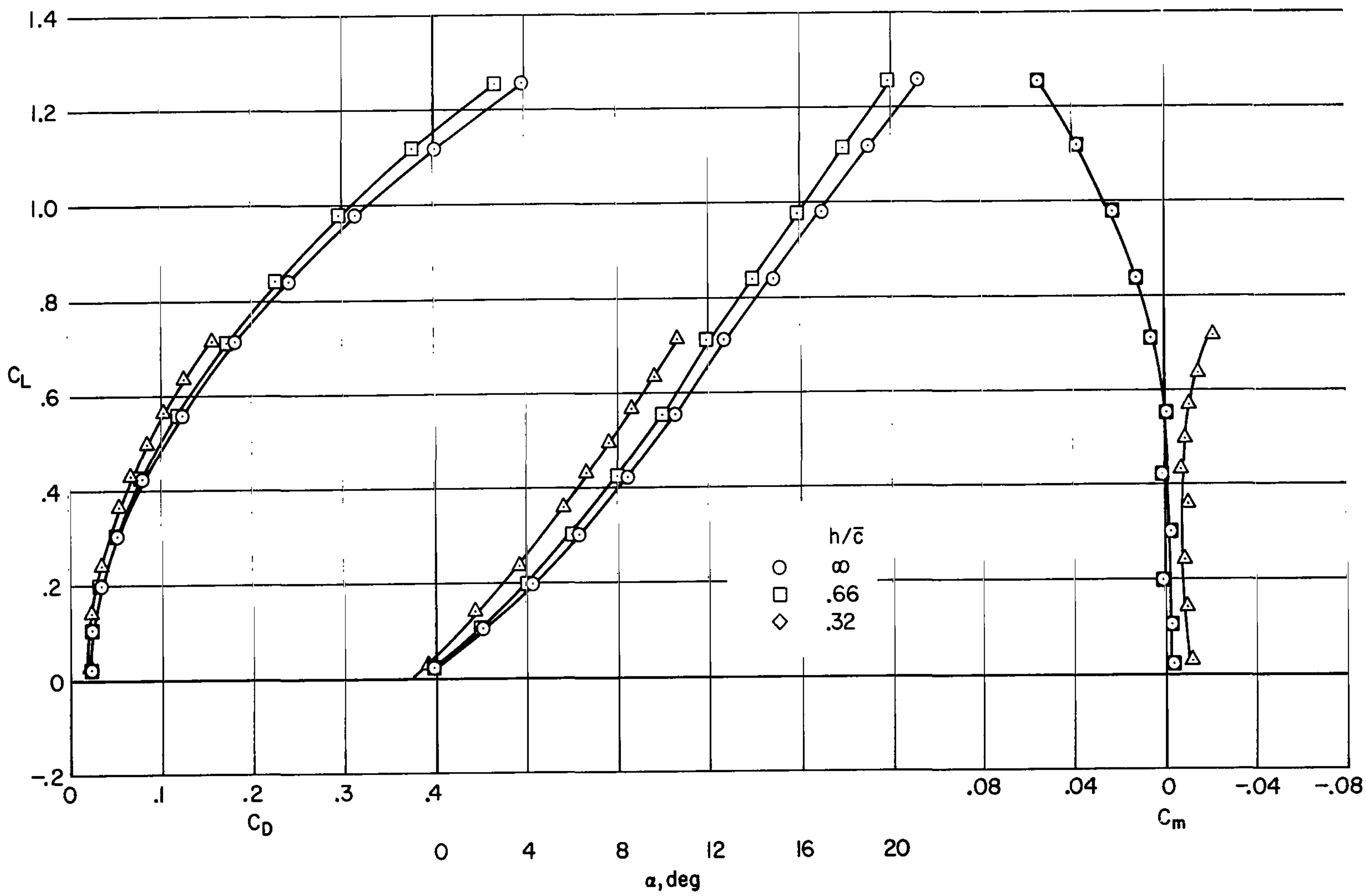

Figure 15.- The effect of ground proximity on the model with the larger 77° strakes; A = 1.34, tips off, $\delta_n = 0^\circ$, $\delta_f = 0^\circ$.

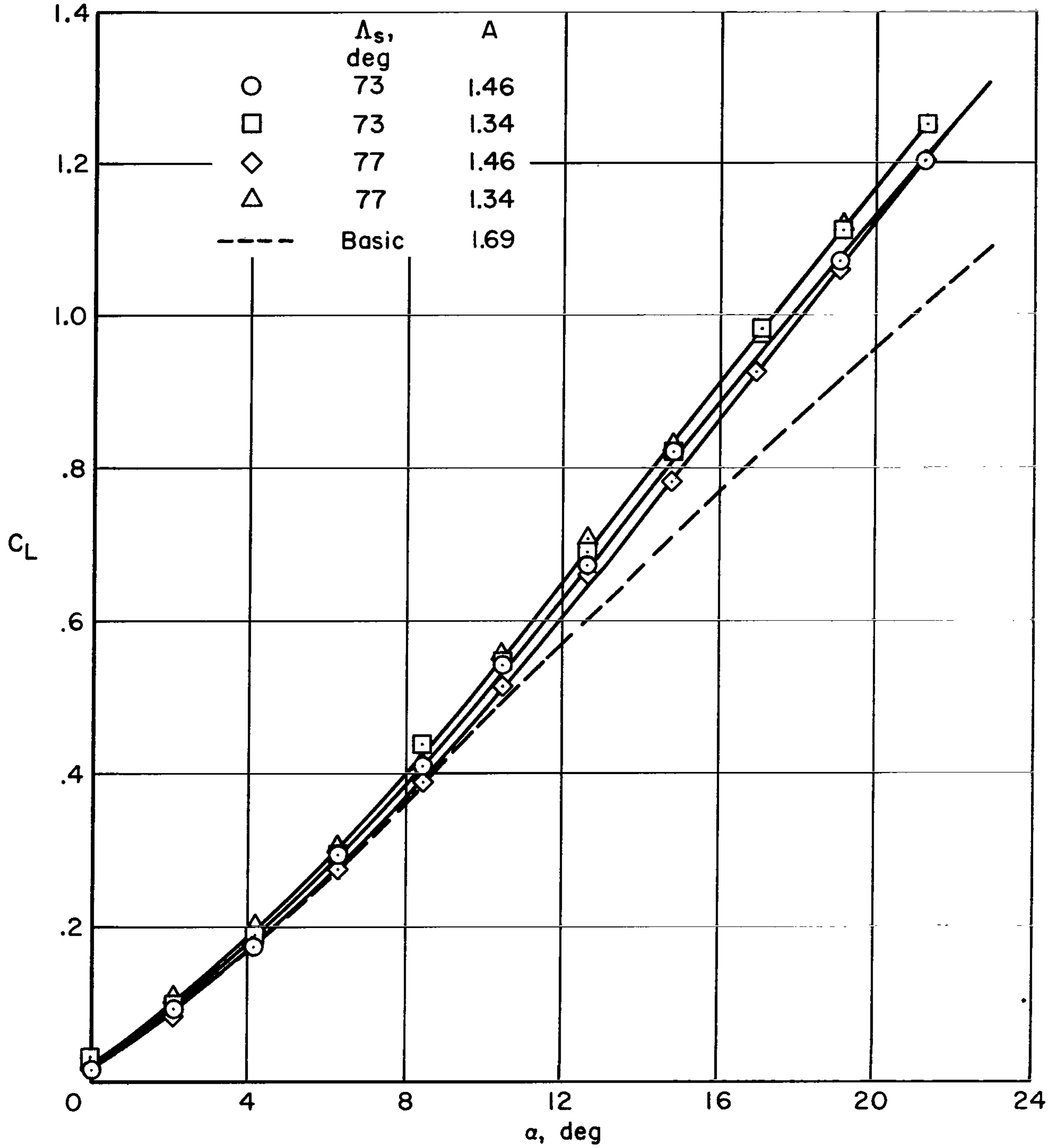

(a) $\delta_n = 0^{\circ}$

Figure 16.- The effect of strakes on lift; $\delta_f = 0^{\circ}$, tips off, $h/\bar{c} \rightarrow \infty$.

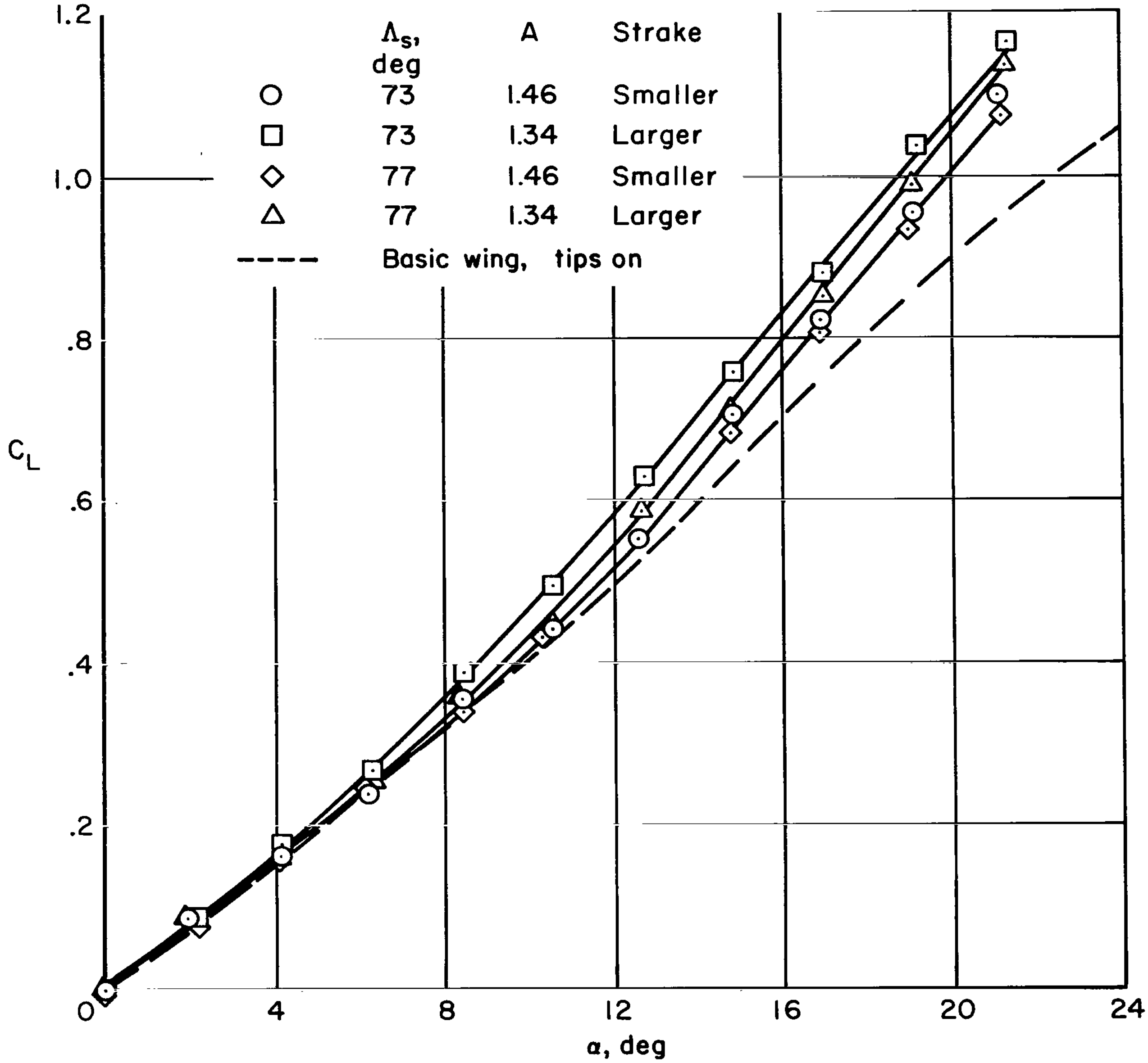

(b) $\delta_n = 30^\circ$, partial span.

Figure 16.- Concluded.

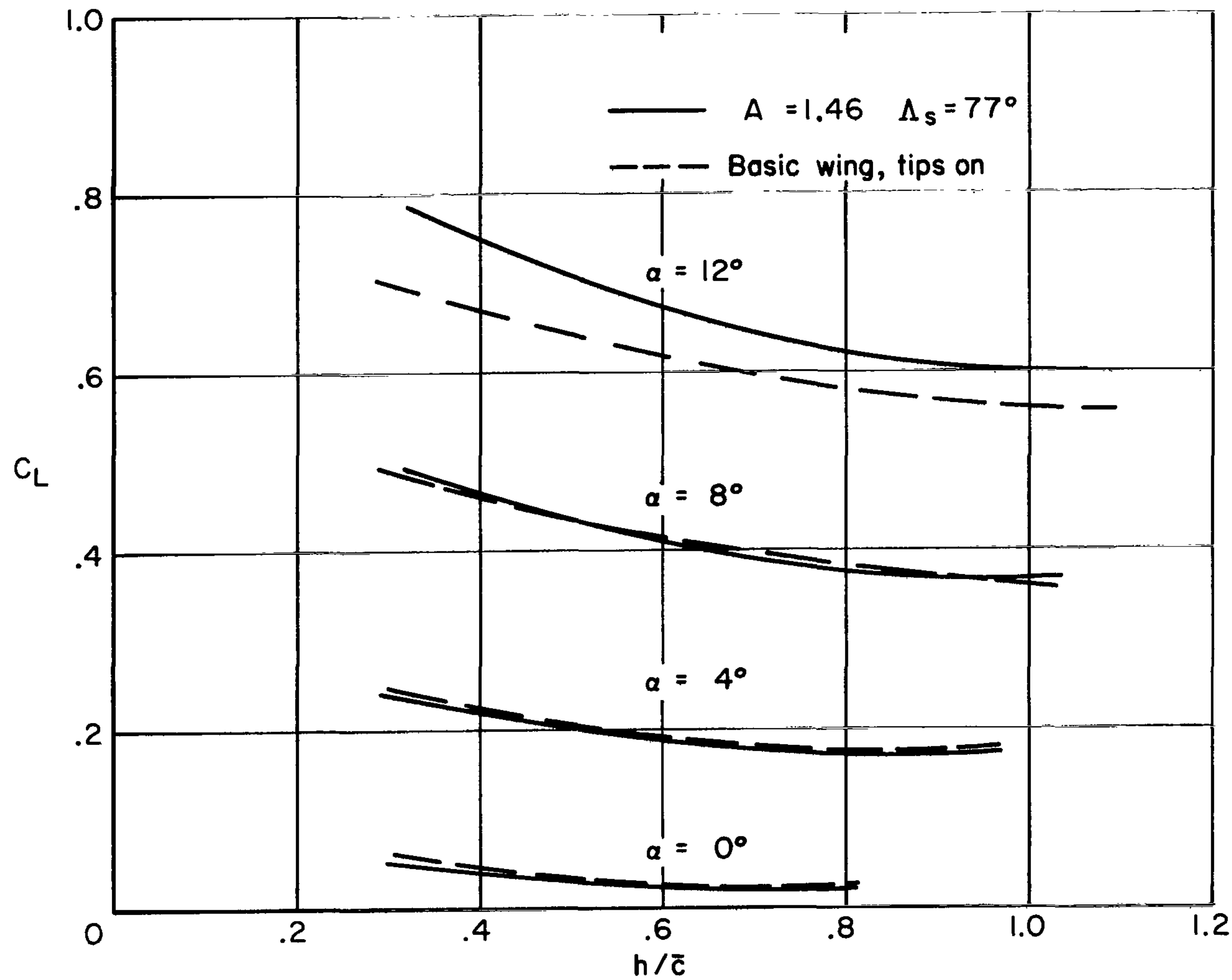

Figure 17.- The effect of ground proximity on lift; $\delta_n = 0^\circ$, $\delta_f = 0^\circ$.

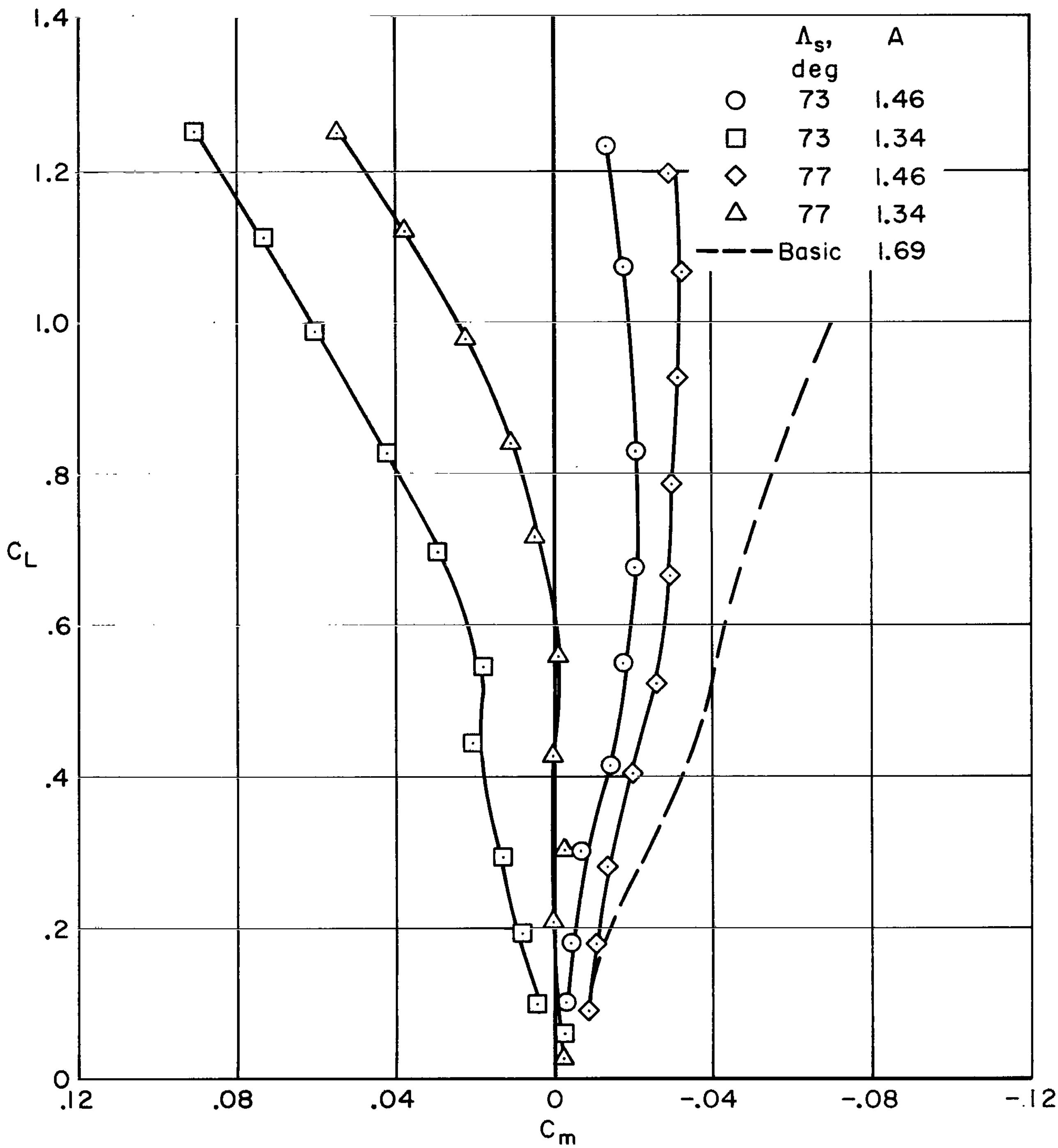

(a) $\delta_n = 0^\circ$

Figure 18.- The effect of strakes on pitching moment; $\delta_f = 0^\circ$, tips off, $h/\bar{c} \rightarrow \infty$.

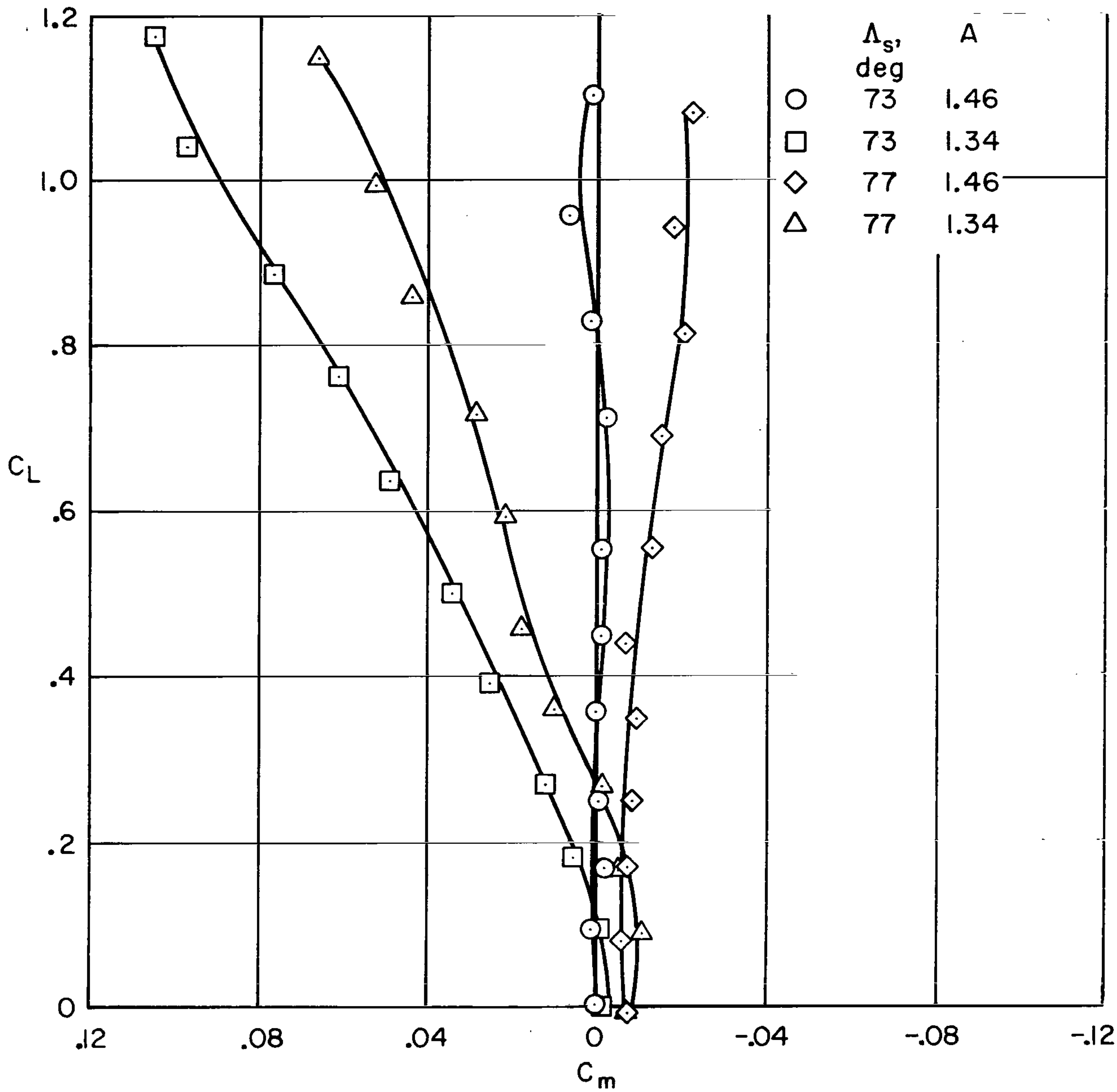

(b) $\delta_n = 30^\circ$; partial span.

Figure 18.- Concluded.

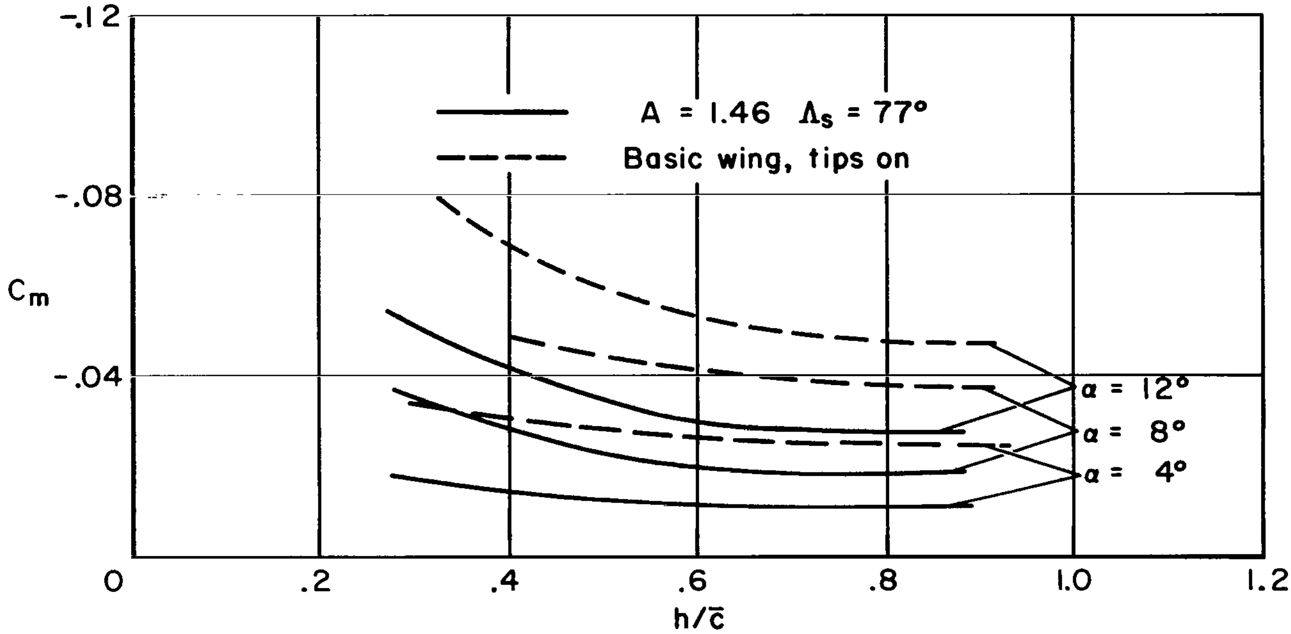

Figure 19.- The effect of ground proximity on pitching moment; $\delta_n = 0^\circ$.

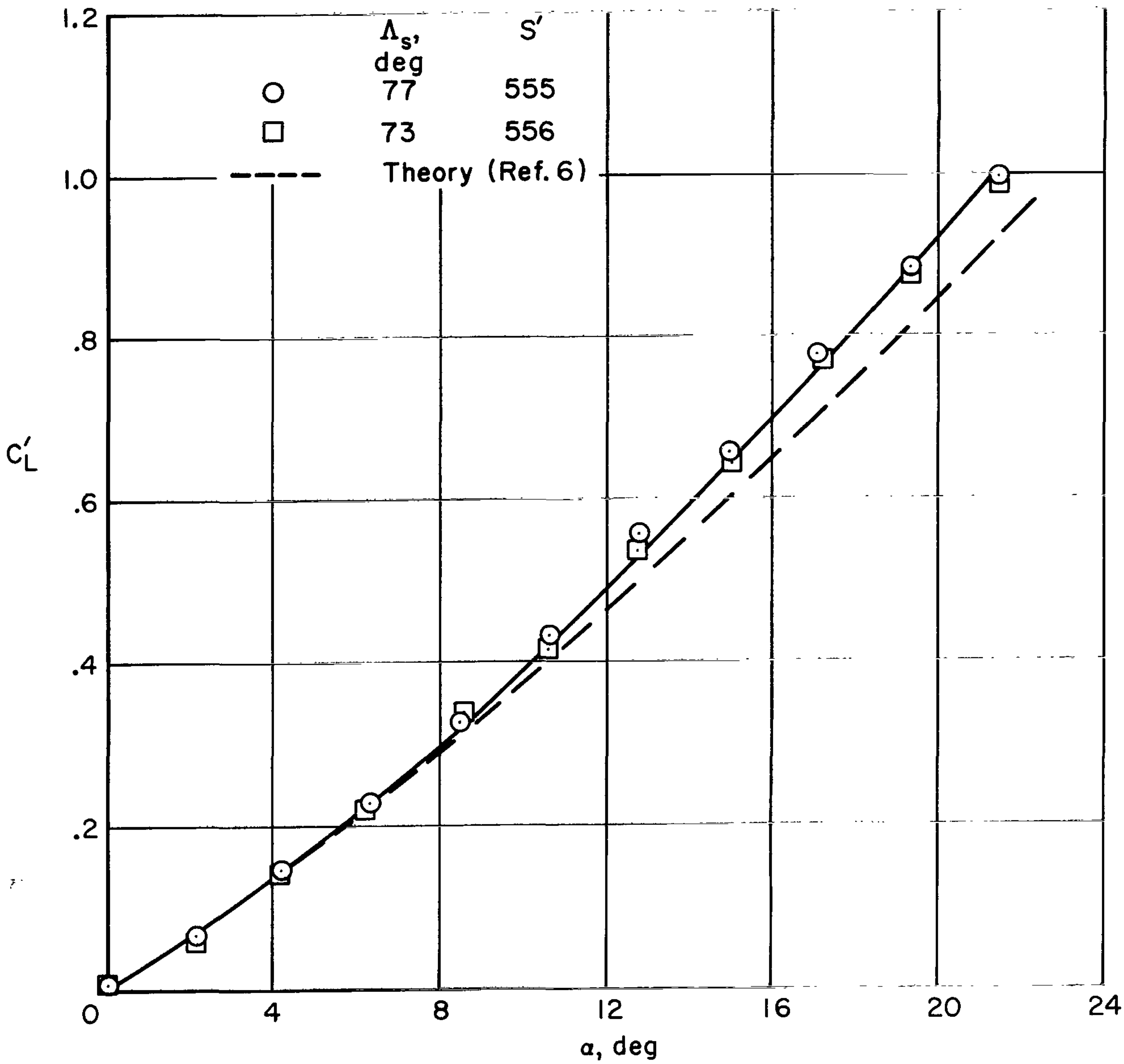

(a) Aspect ratio = 1.34, larger strake.

Figure 20.- Comparison of theory with experimental results for the basic wing and the smaller and larger strakes; $\delta_n = 0^\circ$, $\delta_f = 0^\circ$, tips off, $h/\bar{c} \rightarrow \infty$.

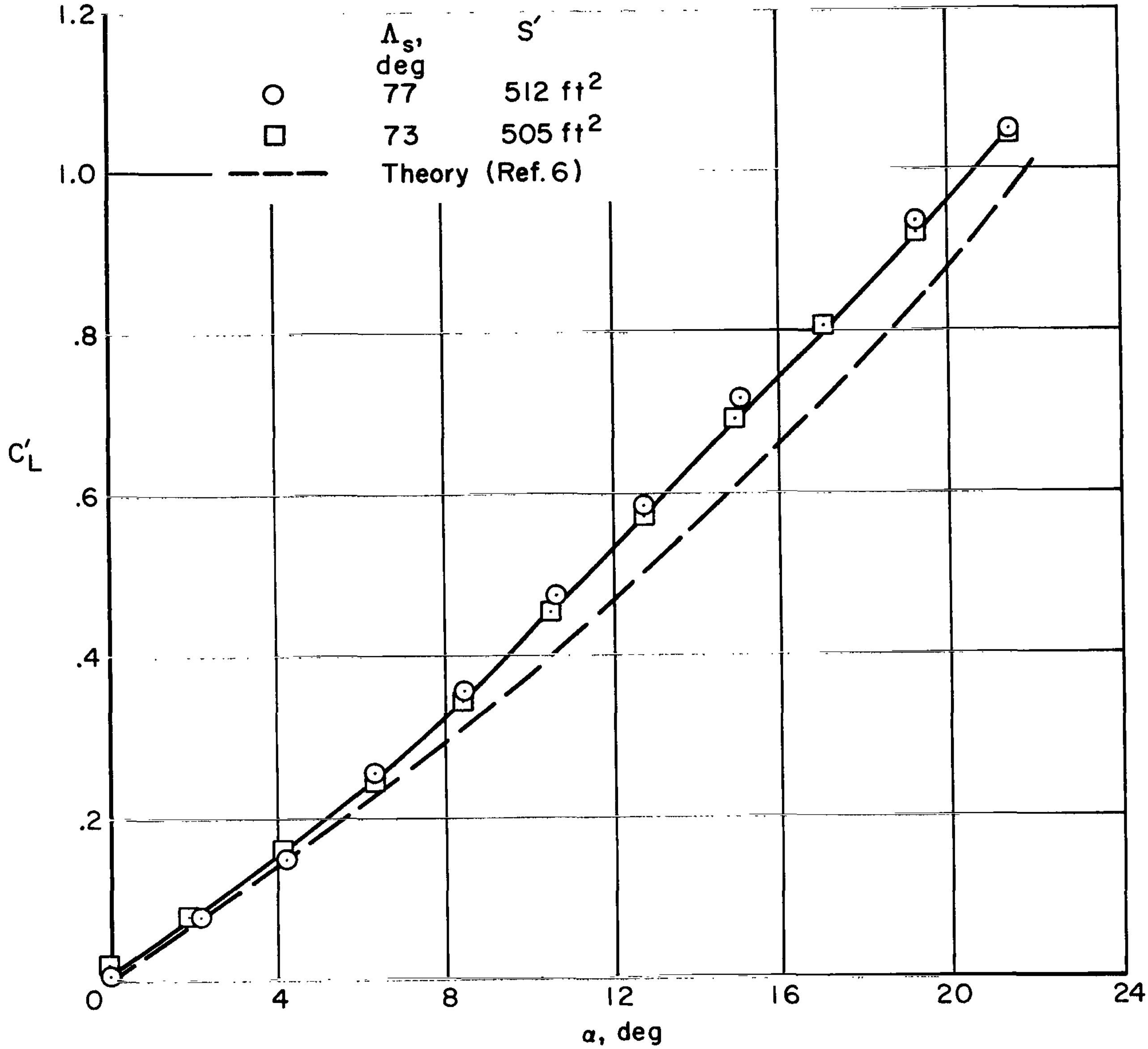

(b) Aspect ratio = 1.46, smaller strake.

Figure 20.- Continued.

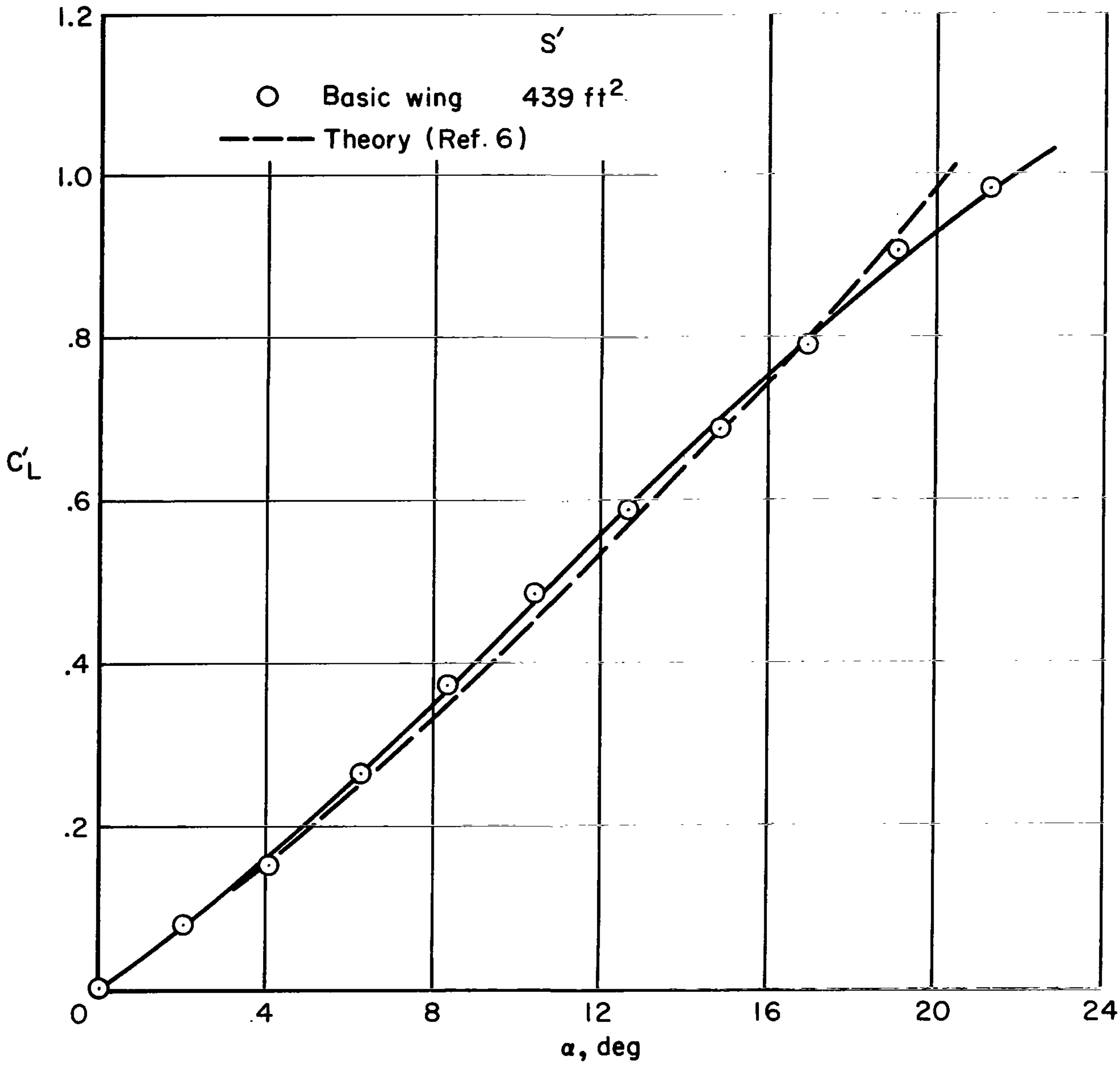

(c) Aspect ratio = 1.69, basic wing.

Figure 20.- Concluded.

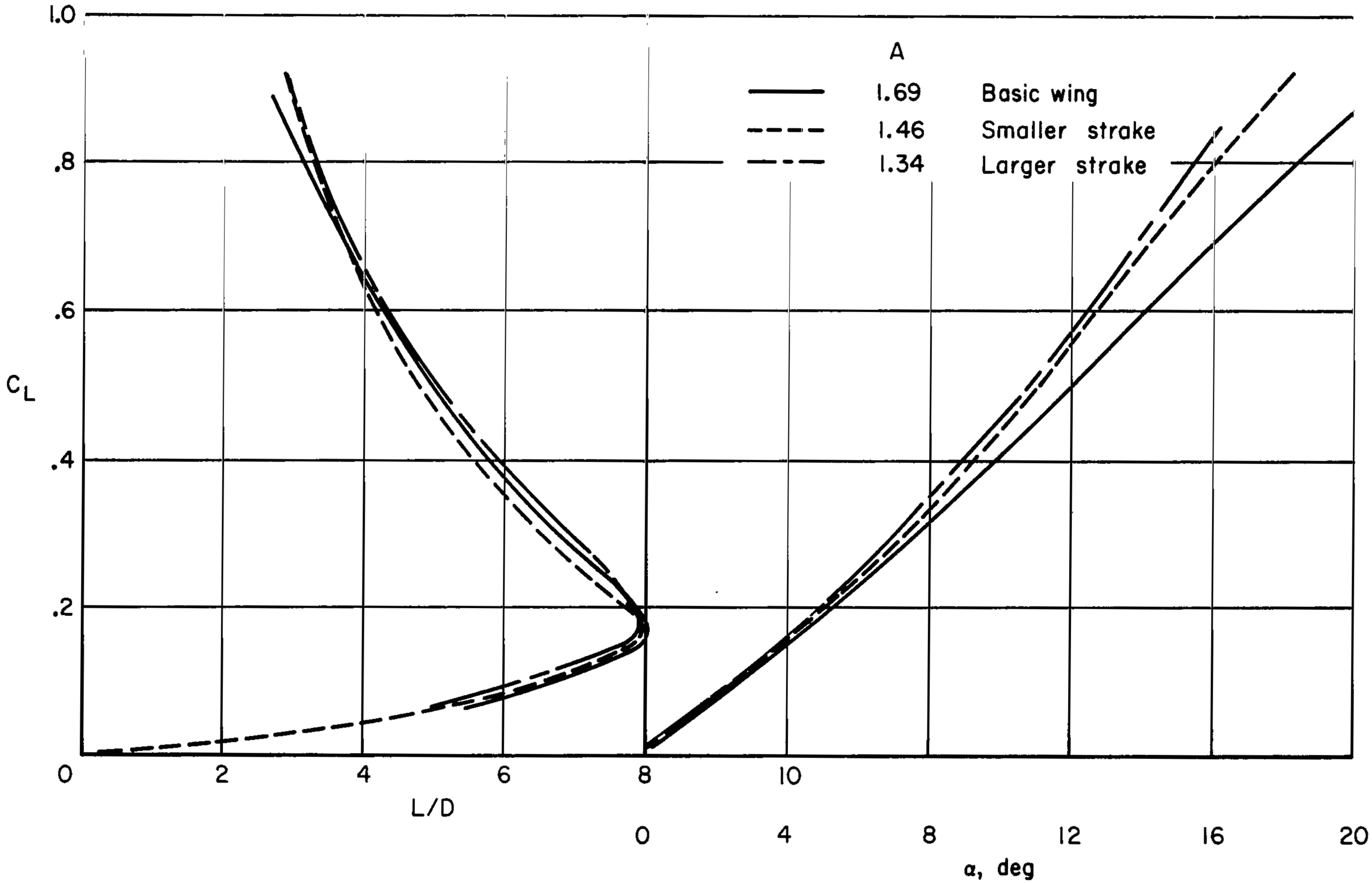

(a) $\delta_n = 0^\circ$, $\Lambda_s = 73^\circ$

Figure 21.- The characteristics of the model with strakes, trimmed for a static margin of 4 percent by means of elevons, tips off, $h/\bar{c} \rightarrow \infty$.

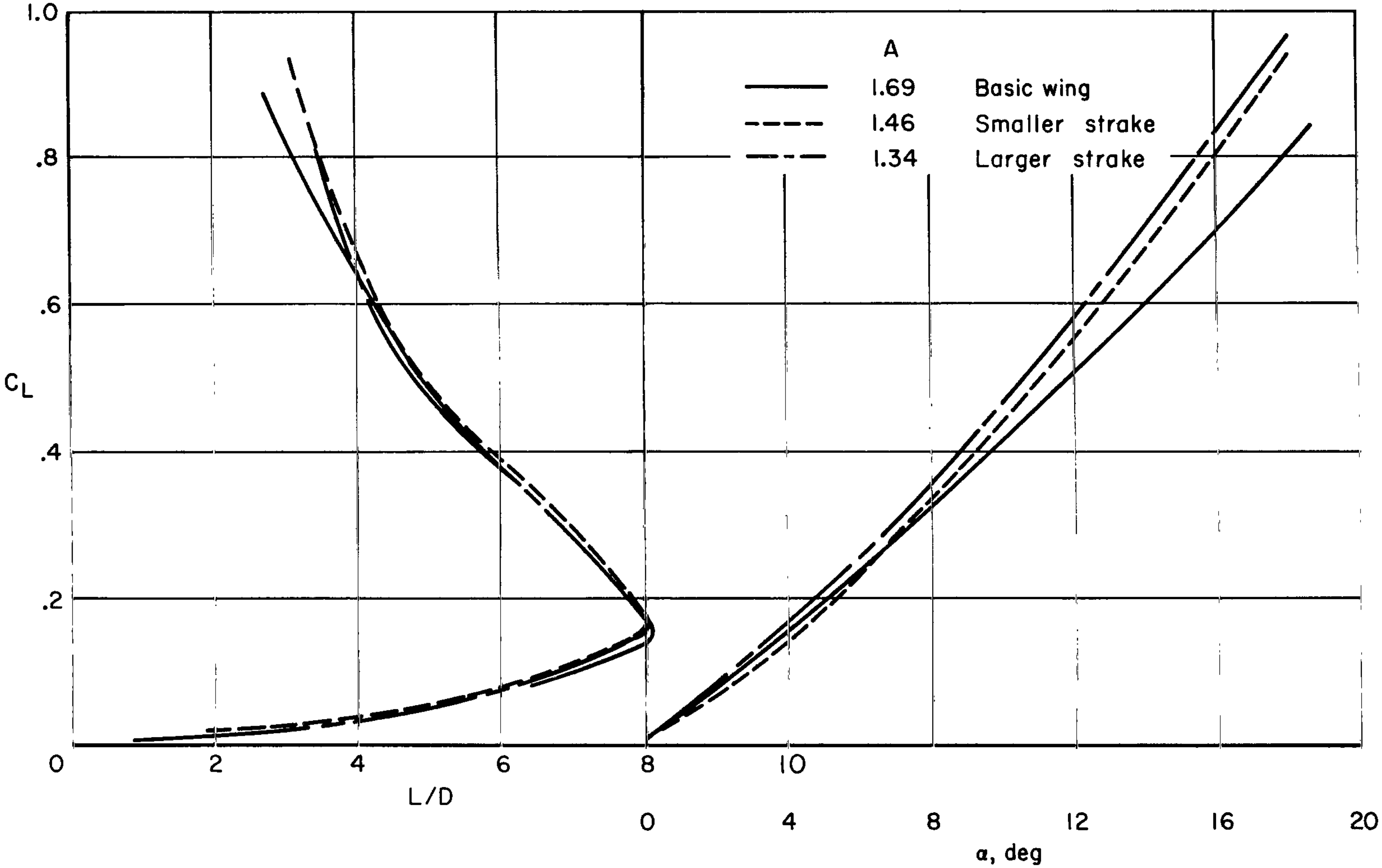

(b) $\delta_n = 0$, $\Lambda_s = 77^o$.

Figure 21.- Continued.

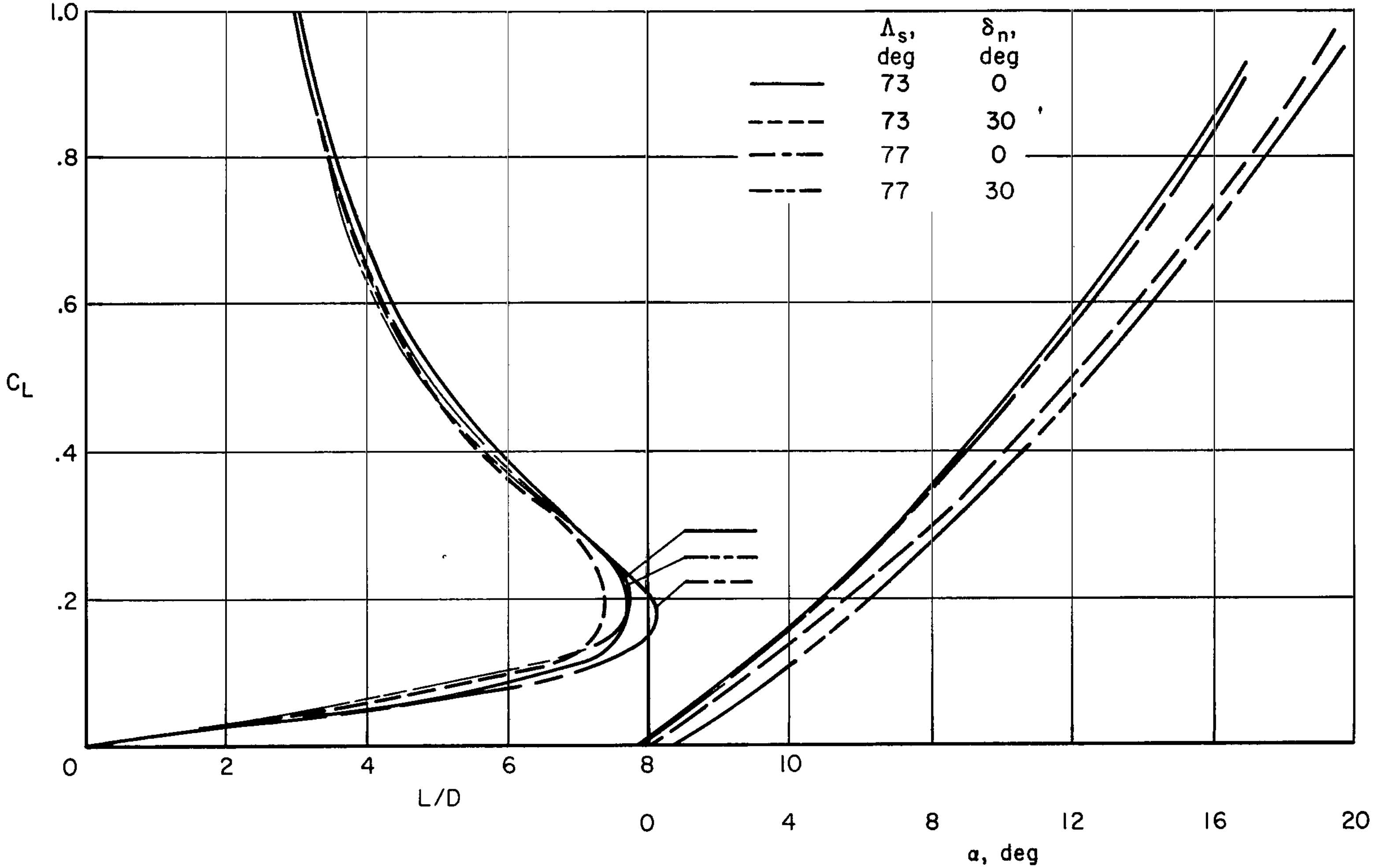

(c) A = 1.34, larger strake, partial span.

Figure 21.- Continued.

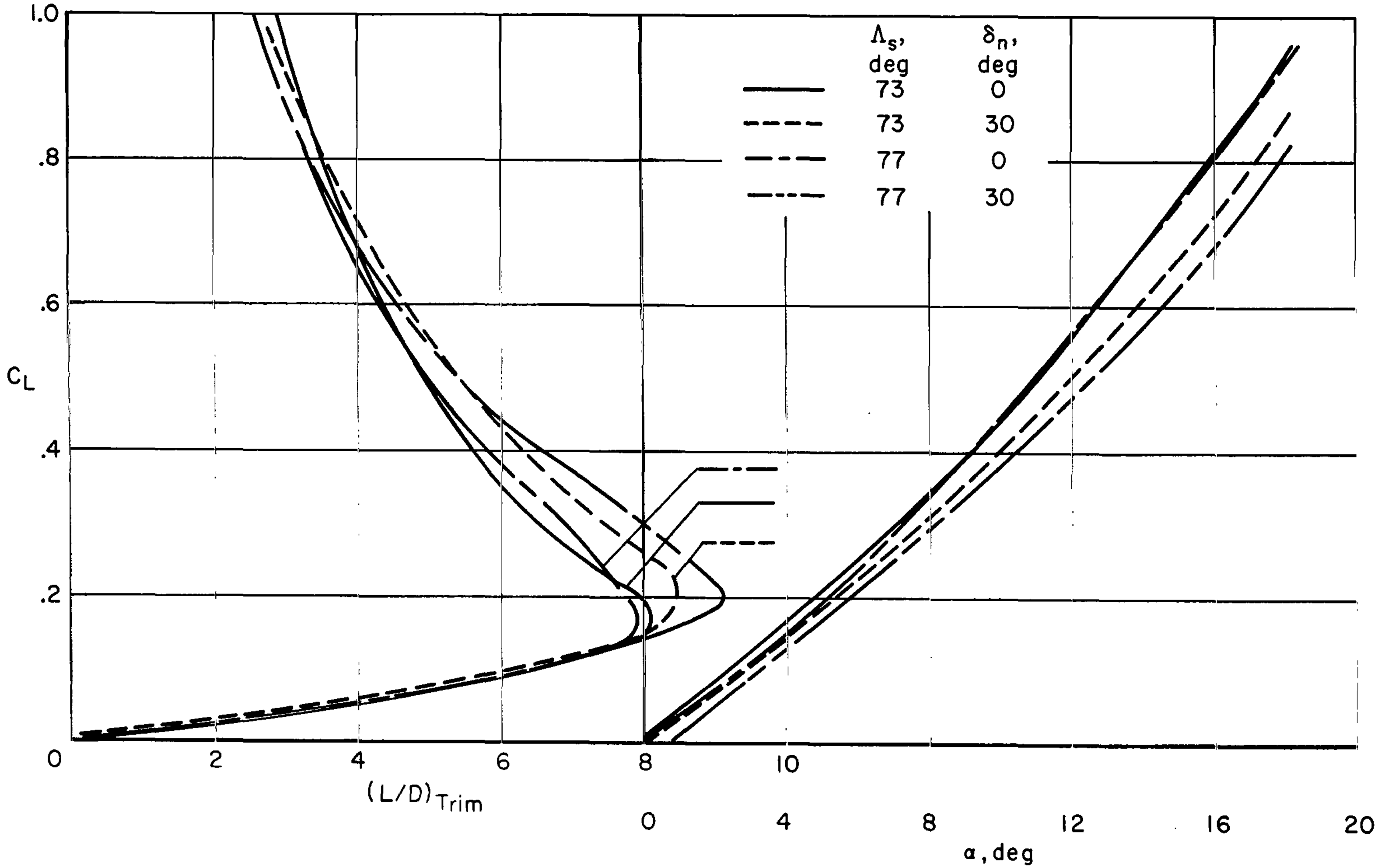

(d) A = 1.46, smaller strake, partial span.

Figure 21.- Concluded.

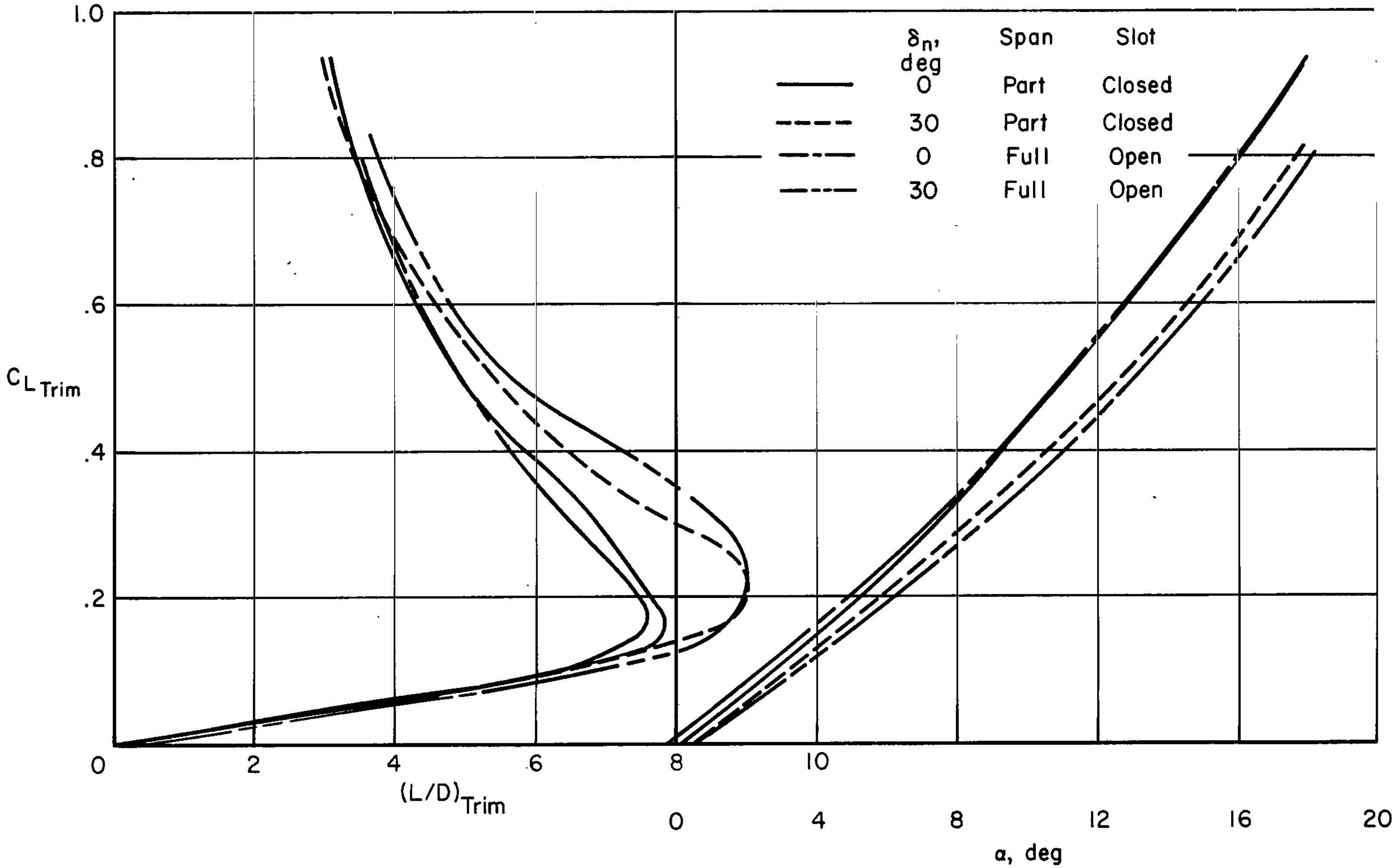

Figure 22.- The effect of full-span leading-edge flaps and slots on the trimmed characteristics of the model with the smaller 77° strakes; A = 1.46, static margin = 4 percent, tips off, $h/\bar{c} \rightarrow \infty$, elevon controlled.

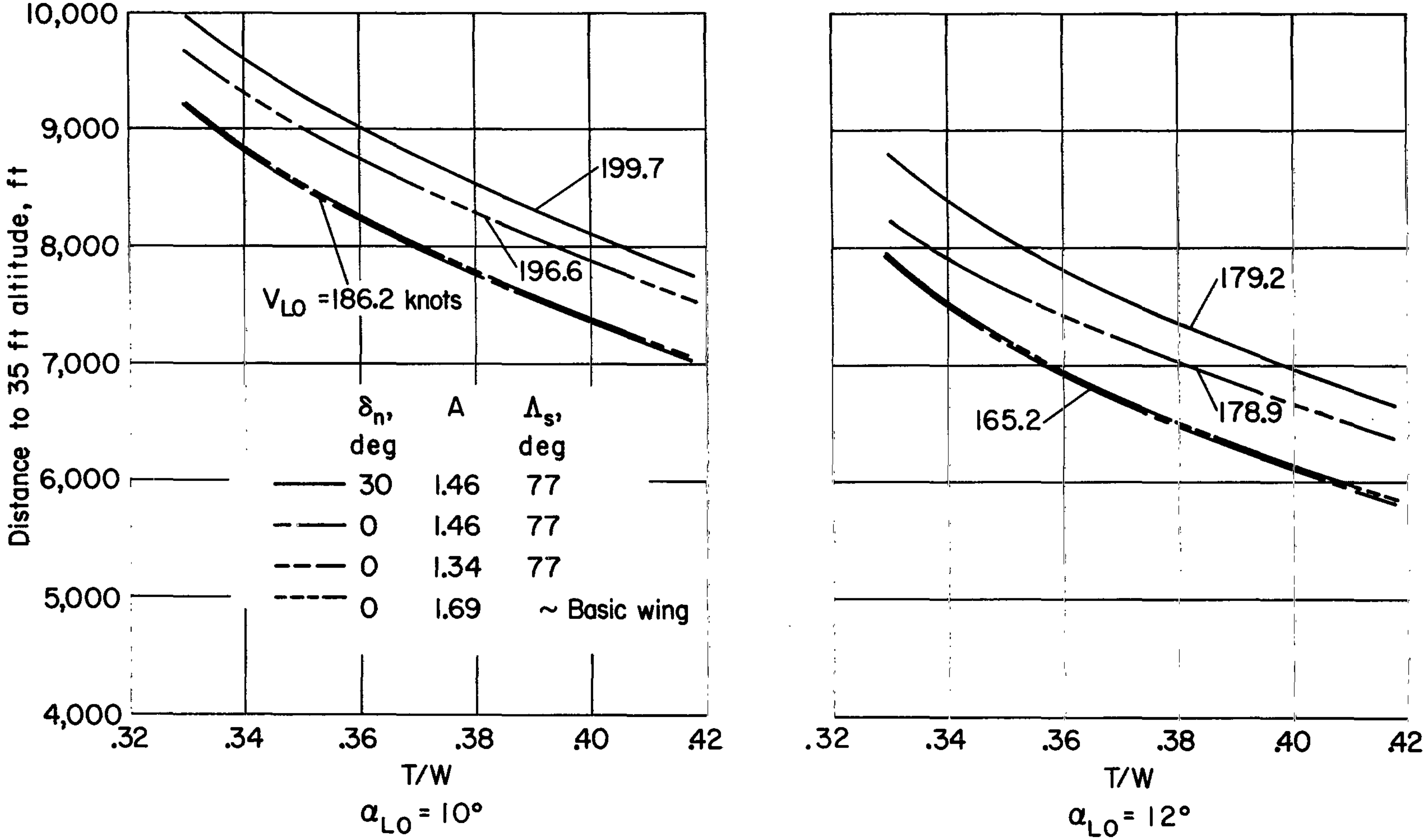

Figure 23.- The effect of strakes on the take-off distance required to reach an altitude of 35 ft; W/S = 70 psf, W = 450,000 lb.

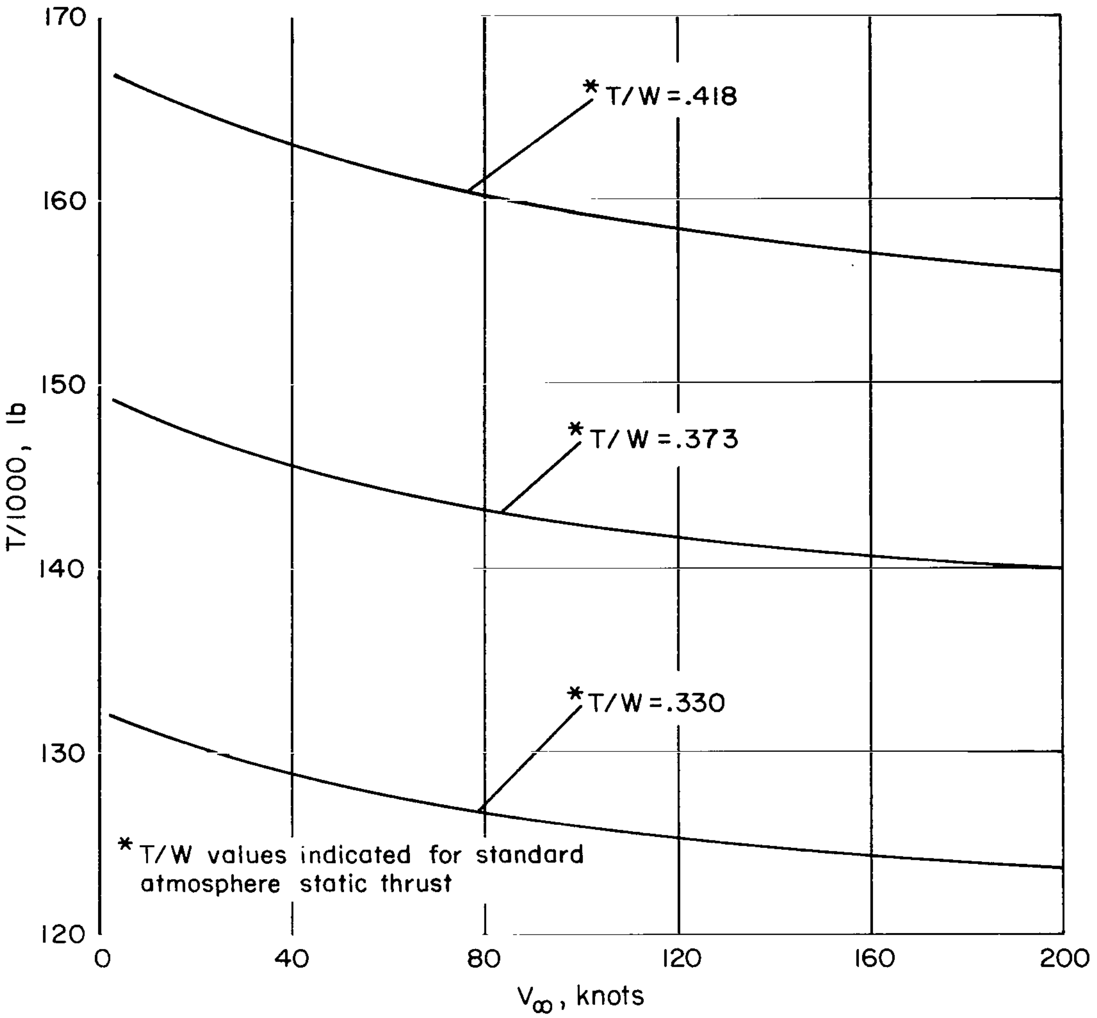

Figure 24.- The variation of hot-day thrust with airspeed used in calculation of the ground roll and take-off distances presented in figure 23; W = 450,000 lb.

"The aeronautical and space activities of the United States shall be conducted so as to contribute . . . to the expansion of human knowledge of phenomena in the atmosphere and space. The Administration shall provide for the widest practicable and appropriate dissemination of information concerning its activities and the results thereof."

—NATIONAL AERONAUTICS AND SPACE ACT OF 1958

NASA SCIENTIFIC AND TECHNICAL PUBLICATIONS

TECHNICAL REPORTS: Scientific and technical information considered important, complete, and a lasting contribution to existing knowledge.

TECHNICAL NOTES: Information less broad in scope but nevertheless of importance as a contribution to existing knowledge.

TECHNICAL MEMORANDUMS: Information receiving limited distribution because of preliminary data, security classification, or other reasons.

CONTRACTOR REPORTS: Technical information generated in connection with a NASA contract or grant and released under NASA auspices.

TECHNICAL TRANSLATIONS: Information published in a foreign language considered to merit NASA distribution in English.

TECHNICAL REPRINTS: Information derived from NASA activities and initially published in the form of journal articles.

SPECIAL PUBLICATIONS: Information derived from or of value to NASA activities but not necessarily reporting the results of individual NASA-programmed scientific efforts. Publications include conference proceedings, monographs, data compilations, handbooks, sourcebooks, and special bibliographies.

Details on the availability of these publications may be obtained from:

SCIENTIFIC AND TECHNICAL INFORMATION DIVISION

NATIONAL AERONAUTICS AND SPACE ADMINISTRATION

Washington, D.C. 20546